

Post Access Report

Acoustic Particle Velocity Measurements around a Tidal Current Turbine

Awardee: University of Washington

Awardee point of contact: Brian Polagye

Facility 1: Integral Consulting

Facility point of contact: Kaus Raghukumar

Facility 2: Pacific Northwest National Laboratory

Facility point of contact: Nichole Sather

Date: 12/30/2024



Testing & Expertise for Marine Energy

1 EXECUTIVE SUMMARY

Quantifying the underwater sound produced by tidal turbines is essential both to understand their potential environmental impacts and to understand how that sound might interfere with the intended application of the turbine (e.g., powering acoustic monitoring systems). In this project, we measured the sound radiated by a small-scale crossflow tidal turbine. The turbine was deployed from October 2023 to March 2024 in the tidal channel at the entrance to Sequim Bay, WA. Acoustic measurements were made with three different sensor packages: a commercial-off-the-shelf vector sensor (operated by PNNL), a vector sensor array (operated by Integral Consulting), and drifting hydrophones (operated by UW). Acoustic recordings from the three sensors highlight changes in the turbine acoustic signature over the course of a tidal cycle and throughout the 6-month turbine deployment. Our results also highlight the utility of acoustic vector sensors for localizing sound attributable to marine energy devices in acoustically complex environments.



Testing & Expertise for Marine Energy

2 INTRODUCTION TO THE PROJECT

University of Washington (UW) deployed a cross-flow turbine system, referred to as the “Turbine Lander”, on a gravity-anchored seabed lander in the entrance channel to Sequim Bay, adjacent to Pacific Northwest National Laboratory’s (PNNL) Marine and Coastal Research Laboratory. PNNL and Integral Consulting (Integral) deployed acoustic vector sensing systems around the Turbine Lander to produce directionally-resolved estimates of the sound produced by the turbine system, and UW conducted concurrent surveys with drifting hydrophones. The objectives of this test were to:

1. Attribute sound sources to the turbine to inform future use of the system as a power source for environmental studies or defense applications;
2. Broaden the general understanding of radiated noise from marine energy converters;
3. Compare concurrent measurements of tidal turbine sound using vector sensors and pressure-sensitive hydrophones; and,
4. Benchmark the new acoustic particle motion measurement capability at the PNNL TEAMER facility.

3 ROLES AND RESPONSIBILITIES OF PROJECT PARTICIPANTS

3.1 Applicant Responsibilities and Tasks Performed

UW was responsible for deploying and operating the Turbine Lander and conducting concurrent drifting hydrophone measurements while the PNNL and Integral vector sensors were deployed. UW provided the drifting hydrophone systems (Drifting Acoustic Instrumentation SYstem; DAISY). UW also provided PNNL and Integral with a log of turbine operating states and time series of all turbine performance parameters to correlate with acoustic measurements. UW collaborated with both facilities on comparative data analysis and will collaborate with the facilities on a scholarly publication describing the test and results.

3.2 Network Facilities Responsibilities and Tasks Performed

PNNL prepared their vector sensor, deployed it and the NoiseSpotter® adjacent to the turbine, and analyzed measurement data. PNNL also provided research vessels, vessel operators, and scientific diver support for deployment and recovery of the PNNL and Integral acoustic vector sensors and the UW drifting hydrophones.

Integral prepared the NoiseSpotter® for deployment, participated in deployment and recovery operations, and analyzed measurement data.

Both facilities collaborated with UW on comparative data analysis and will collaborate with UW on a scholarly publication detailing the test and results.

4 PROJECT OBJECTIVES

The project had four objectives:

- **Quantify sound generated by the turbine and identify the sources of generated sound:** Attribution of sound sources to the turbine and identification of the source is important for future use of the Turbine Lander platform for environmental studies where such sound could bias observations or defense applications where radiated noise signatures would reveal its presence. Three-dimensional bearing estimates enabled by an array of particle motion sensors can help identify and geolocate a variety of acoustic sources such as boats, ships, marine mammals and submarines.
- **Broaden the general understanding of radiated noise from marine energy converters:** While noise from tidal turbines, particularly turbines at this scale, is not expected to have biologically significant intensity, it remains an environmental concern. Future tidal turbines will require measurements of the acoustic output, coupled with propagation modeling. The demonstration of appropriate technologies to accomplish this remains important in helping inform developers/regulators of available tools. In addition, the effects of acoustic particle motion on fishes and invertebrates is of growing concern. It has been argued that acoustic particle motion is the particular quantity that can affect fishes and invertebrates and there is considerable ongoing research to further investigate its effects (Popper and Hawkins 2019). Characterization of particle motion from tidal turbines can contribute to this body of knowledge.
- **Compare acoustic measurement methods:** To date, there have been no concurrent measurements of turbine sound using vector sensors and hydrophones. This deployment is an opportunity to benchmark comparative measurement techniques and inform the development of international standards for acoustic characterization of marine energy converters.
- **Benchmark the new acoustic particle motion measurement capability at the PNNL TEAMER facility:** This will increase confidence for use in future open water testing at PNNL MCRL site. During this deployment, PNNL will gain experience deploying the sensor and analyzing data outputs.

To achieve these objectives, the facilities deployed two acoustic vector sensors and the applicant deployed drifting hydrophones to measure sound generated by the turbine. Key parameters that were measured included turbine sounds during various phases of device operation (ramp-up, continuous operation under various hydrodynamic current regimes, ramp-down, modes of failure, if any), as well as ambient noise from vessels and other sources of underwater sound.

5 TEST FACILITY, EQUIPMENT, SOFTWARE, AND TECHNICAL EXPERTISE

Testing was conducted at the mouth of Sequim Bay where tidal currents are the strongest (Figure 1). This location is in close proximity to PNNL's Marine and Coastal Research Laboratory (MCRL). PNNL's vessel operators are accustomed to operating in such currents, as well as deployment and recovery considerations for the drifting systems. PNNL's small boats (e.g., R/V Desdemona) are ideal for deployment of drifting sensors because they offer sufficient deck space for instrument staging and a low, continuous freeboard that facilitates instrument deployment and recovery. PNNL personnel led field operations, including vessel operation and diving.

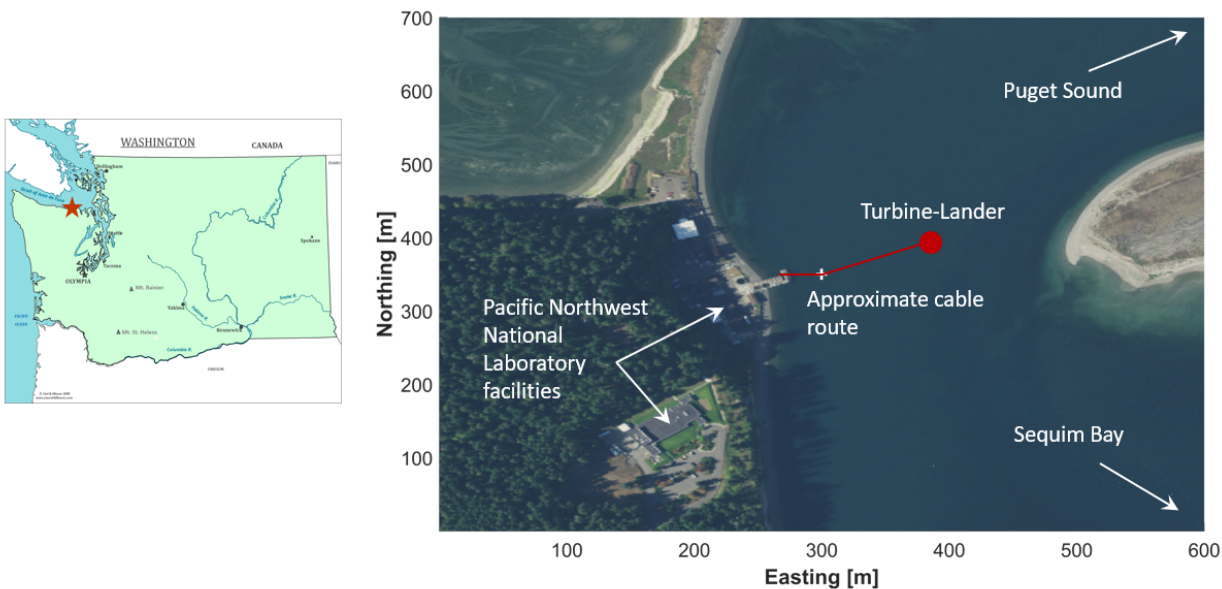


Figure 1: Turbine deployment site in Sequim Bay, WA

Integral has developed and demonstrated the NoiseSpotter®, a passive acoustic sensing device capable of measuring acoustic pressure and particle motion. A number of early NoiseSpotter® field trials occurred in Sequim Bay, leading to significant experience working in the area. The NoiseSpotter® has since demonstrated the ability to make measurements in high-flow areas, and of low intensity sounds such as those produced by marine energy converters.

Integral personnel included Dr. Kaustubha Raghukumar, Mr. Frank Spada, and Dr. Grace Chang. All three personnel have extensive expertise in oceanographic deployments. Dr. Raghukumar and Mr. Spada are part of the original NoiseSpotter® development team and have conducted five NoiseSpotter® deployments in Sequim Bay to date.

PNNL's Marine and Coastal Research Laboratory in Sequim, WA (PNNL) has extensive experience making acoustic measurements in high energy environments, particularly in and around the test site at Sequim



Testing & Expertise for Marine Energy

Bay. PNNL acquired a particle motion sensor in 2022 intended for monitoring acoustic particle motion at marine energy sites, and recently designed a deployment platform for this sensor. Preliminary testing of the sensor was successfully conducted in quiescent waters of Sequim Bay in January 2023.

Key PNNL personnel include Dr. Emma Cotter and Dr. Joe Haxel, both of whom have extensive experience deploying oceanographic equipment in and around Sequim Bay and performing acoustic data analysis. PNNL personnel will also be supported by the PNNL vessel operations and dive teams, led by Dr. John Vavrinec.

Integral conducted data processing and analysis in Python, while PNNL and UW conducted data processing in MATLAB. This leveraged Integral's existing code base for vector sensor data processing and UW's existing code base for drifting hydrophone data processing. PNNL developed vector sensor data processing code in MATLAB because project staff have more experience in this programming language. Data files were shared between UW, Integral, and PNNL as binary MATLAB or netcdf files that can be readily parsed in either programming language.

6 TEST OR ANALYSIS ARTICLE DESCRIPTION

The Turbine Lander (Figure 2) was deployed in the entrance channel to Sequim Bay, adjacent to PNNL's Marine & Coastal Research Laboratory (Figure 1, 48° 4.79' N, 123° 2.60' W) from October 2023 to March 2024. The turbine rotor was 1.2 m high and 0.85 m in diameter with four, straight blades. The rotor was indirectly connected to a permanent magnet generator by a magnetic coupling. The in-air weight was approximately 2400 kg. During this demonstration, any power generated was sent to a resistive load dump, but future deployments may allow autonomous operation for powering oceanographic sensing packages or underwater vehicle recharge. For this reason, it is important to understand the noise radiated by the turbine and its sources.

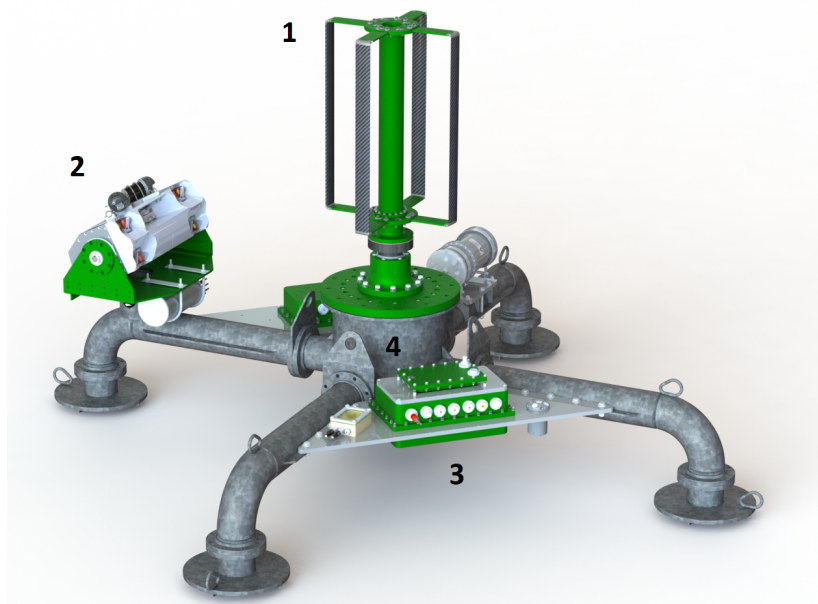


Figure 2: Schematic rendering of the Turbine Lander. Key components include (1) the rotor, (2) the LAMP - an environmental sensing package, (3) the housings for the power electronics and dump load, and (4) generator, which is located inside the center of the lander structure. Additional components that are either not labeled or shown include the shore cable junction bottle (located beneath the LAMP), shore cable itself, and a prototype hydrophone array (front, right leg).

Pre-deployment dockside testing conducted by UW identified three probable sound sources associated with operation of the turbine. The first was a continuous tone at 4 kHz that was present whenever the power electronics are energized, regardless of whether or not the turbine was rotating. The second was a tone at 8 kHz that was present when the turbine was rotating and likely associated with the generator. The third consisted of a tone and harmonics that varied linearly in proportion to rotation rate and likely attributable to the bearing pack that supports the rotor. However, during this dockside testing, the turbine was rotated by the servomotor and did not experience a thrust load. As a result, it was anticipated that the sound generated by the turbine would differ during the Sequim Bay deployment.



Testing & Expertise for Marine Energy

In addition to dockside testing, during vessel-based testing in April 2022, UW conducted drifting measurements around the turbine using DAISYs. Due to the presence of mooring lines to secure the test vessel, DAISY proximity was limited to 100 m and only traces of expected sounds could be identified. This was likely due to a combination of proximity to the source, potential differences between motored and powered turbine operation, and relatively high levels of ambient noise from other sources (e.g., a diesel generator on board the test vessel, moorings). Using localization with multiple DAISYs, it might be possible to differentiate between turbine sound and sources of ambient noise. However, the accuracy of this localization depends on multiple factors such that the directional sensing capability from acoustic vector sensors could provide additional insight into sound sources on the turbine.

7 WORK PLAN

7.1 Experimental Setup

The original test plan called for a two-week deployment of the vector sensors at the mouth of Sequim Bay, where the PNNL facility is located. Figure 3 shows the deployment location of the UW tidal turbine and the planned deployment locations of the PNNL vector sensor and NoiseSpotter® over the experiment duration. The two vector sensor systems were to be deployed at multiple locations at a distance of 100 m from the UW tidal turbine, in water depths ranging from 6.8 m to 7.8 m (Table 1). Initially (Day 1), the two systems were to be co-located at location L1, at a bearing of 280° to the turbine (i.e. the vector sensors were due west of the turbine). The PNNL vector sensor was to be redeployed in the same position at location L1 on Days 2-7, while the NoiseSpotter® was to be moved to location L2 on Day 2. The PNNL vector sensor was to be recovered on Day 7, and the NoiseSpotter® was to be recovered and redeployed at location L3 for measurements over Days 8-14. These locations were selected to facilitate directional processing using joint processing of data gathered at L1 and L2. Sound from the tidal turbine is expected to be isotropic (i.e., no azimuthal variability other than propagation effects) since all sound-producing features are of dimensions less than the inverse of acoustic wavelengths being measured. NoiseSpotter® measurements at location L3 were intended to be used to confirm the isotropic nature of sound production by the tidal turbine. In addition to deployed vector sensors, surveys with drifting hydrophones (DAISYs) were intended to complement the stationary measurements.

The team was forced to deviate from the original deployment plan due to unanticipated equipment loss. The original version of the NoiseSpotter® (v1) was deployed as planned on November 8 near L2, but was not found by divers when recovery was attempted on November 17. Recovery efforts and lessons learned are detailed in Section 7.2. Integral had already begun build-out of a new, updated version of NoiseSpotter® (v2) for other efforts, so, after assessing the risks of redeployment and completing testing of NoiseSpotter® v2, it was deployed at L1 in February 2024. The PNNL sensor was not concurrently deployed because it was needed for other projects. At this point in the turbine deployment, one turbine blade had failed and biofouling had accumulated on the turbine lander, so it was anticipated that the sound generated by the turbine might have changed from the November recordings. Actual deployment dates and locations are shown in red in Figure 3 and Table 2.

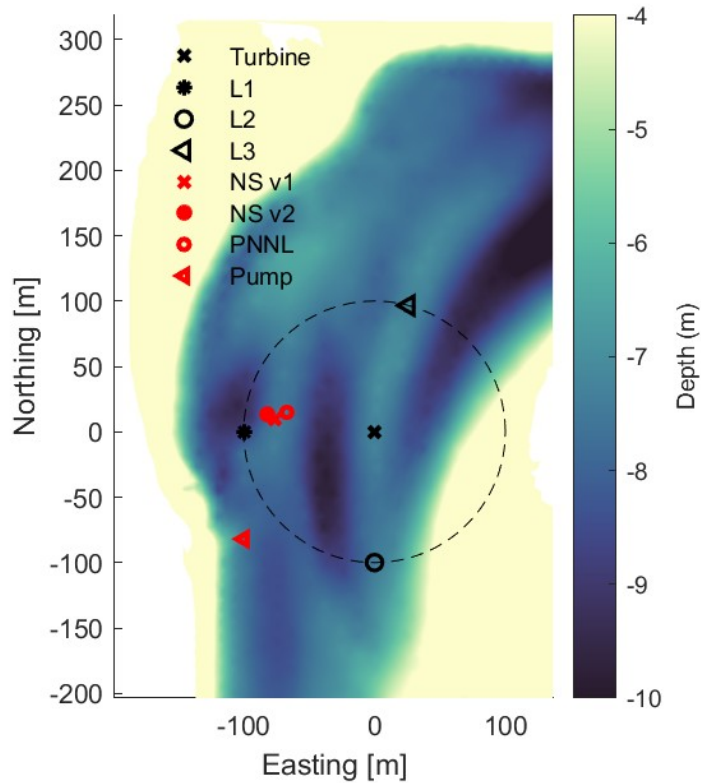


Figure 3: Map of deployment locations showing UW tidal turbine location, planned NoiseSpotter® and PNNL vector sensor location during Day 1 co-located demonstration (L1), planned PNNL vector sensor location on Days 2-7 (L1), planned NoiseSpotter® location on Days 2-7 (L2), and planned NoiseSpotter® location Days 8-14 (L3). The dashed circle indicates a 100 m distance from the UW tidal turbine. Actual deployment locations from which data are reported are indicated in red, as well as the position of the PNNL-Sequim water intake pump, which produced a consistent acoustic signal throughout the dataset.

Table 1: Planned locations and depths of vector sensor deployments

Location	Location	Depth	Duration
Turbine	48.0798°N, 123.0433°W	7.1 m	May 15 - August 15, 2023
L1	48.0795°N, 123.0446°W	7.8 m	Days 1-7
L2	48.0789°N, 123.0431°W	6.8 m	Days 2-7
L3	48.0807°N, 123.0430°W	7.2 m	Days 8-14

Table 2: Actual locations and depths of vector sensor deployments.

Target Location	Actual Location	Sensor(s)	Duration
Turbine	48.0798°N, 123.0433°W	Turbine	October 8, 2023 - March 7, 2024
L1	48.0800°N, 123.0442°W	PNNL Sensor	November 8-17, 2023
L2	48.0799°N, -123.0444°W	NoiseSpotter® v1 ¹	November 8-17, 2023
L2	48.0799°N, 123.0444°W	NoiseSpotter® v2	February 1-14, 2024

¹NoiseSpotter® v1 not recovered; data lost.

7.2 Instrumentation

7.2.1 NoiseSpotter®

The first NoiseSpotter® (v1) deployed was the original configuration constructed out of HDPE rods on a fiberglass grate and was deployed in November 2023. This system was lost following the deployment for reasons still unknown despite extensive efforts to locate it. Subsequently, a second version (v2) was built using a stainless steel cage, which retained the three-dimensional array configuration of the previous version. Both versions are a compact array of three acoustic vector sensors each of which measures acoustic pressure and the three-dimensional particle velocity vector associated with the propagation of an acoustic wave, thereby inherently providing bearing information to an underwater source of sound. Data from all three sensors are synchronously logged by a custom data logger. Time-synchronous data logging allows for coherent processing, but also prevents the system from being broken up into separate parts, necessitating the need for another vector sensing platform, such as the PNNL system (described below) to determine source location. Both NoiseSpotter® platforms have a footprint of 1.2 m x 1.2 m and a height of 1 m. Some differences between the two systems are that NoiseSpotter® v1 consisted of two Geospectrum M20-040 sensors along with a M20-105 sensor, while the NoiseSpotter® v2 consists of three M20-040 sensors. The M20-105 sensor includes a digital compass which allows for placing directional estimates into true-earth coordinates as opposed to a sensor frame of reference.

For v1, pressure and particle velocity channels are sampled at 20 kHz, while for v2, they are sampled at 9600 Hz. The nominal pressure sensitivity of the pressure channel at 1 kHz is -179 dB re $V/\mu\text{Pa}$, which, along with the saturation level of the sensors, allows for measurement of sound source levels up to 240 dB re $1 \mu\text{Pa}$ at a distance of 100 m from the sensor. Frequency-specific calibration is applied to each pressure and particle velocity channel, and then transformed into the time-domain. Acoustic pressure measurements are reported in decibels referenced to 1 microPascal (dB re $1 \mu\text{Pa}$) while particle velocity measurements are reported in decibels referenced to 1 meter per second (dB re 1 m/s).

The frequency sensitivity of both versions of the NoiseSpotter® spans the frequency range 50 Hz - 3 kHz (v1) and 10 Hz – 3 kHz (v2), which spans the frequency range of expected blade noise from the turbines that consist of a tone and harmonics that vary linearly in proportion to rotation rate. However, this frequency range does not cover potential tones from the power electronics and generator at 4 kHz and 8 kHz, respectively, which are beyond the range of commercially-proven accelerometer-based vector sensors.

By utilizing an array of three vector sensors, the NoiseSpotter® obtains signal-to-noise ratio gains, which is particularly useful in characterizing sound from low intensity sources such as tidal turbines located in high ambient noise regions. In tidal channels such as Sequim Bay, the strong currents can induce non-acoustic pressure fluctuations that lead to contamination of acoustic signals. Flow noise contamination can be particularly acute with vector sensors due to saturation of the built-in accelerometer signal by energetic flows. To facilitate NoiseSpotter® deployments in energetic environments, a “flow shield” has been developed and previously tested in the Sequim Bay entrance channel. An Aquadopp Current Profiler (Nortek), with a high-resolution firmware that allows for 3D current velocity measurements in 7 mm vertical bins, was included with the v1 for contextual measurements of flow speed. However, this system was lost and NoiseSpotter® v2 did not have a current profiler. Table 3 provides an overview of all vector sensor instrumentation used.

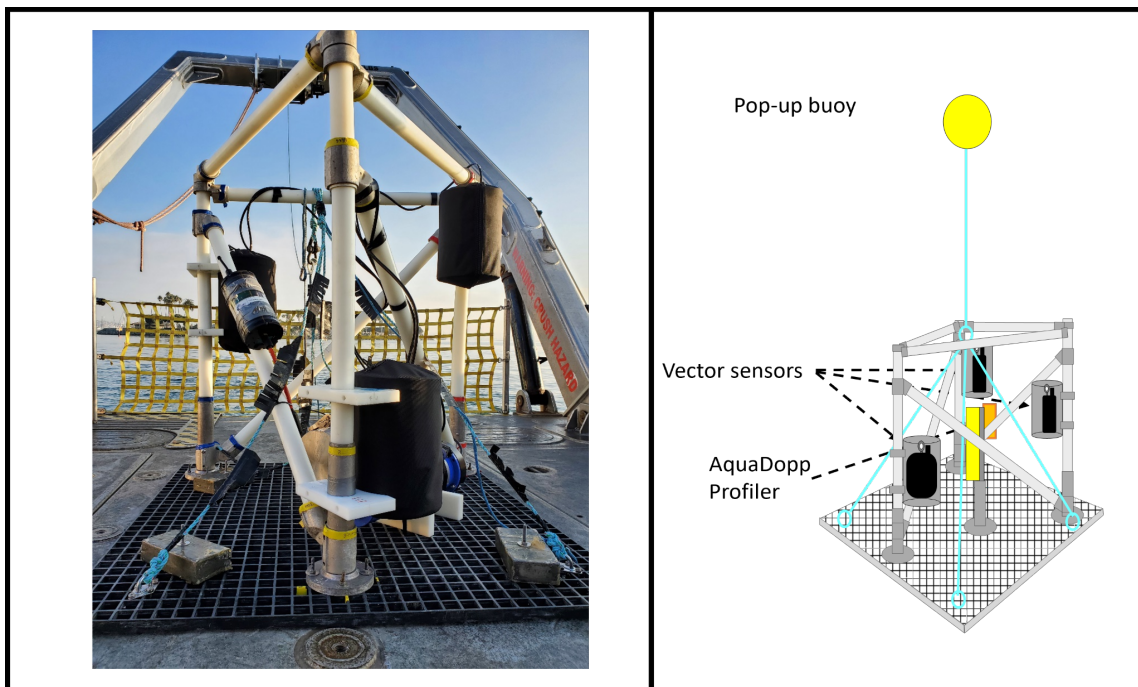


Figure 4: NoiseSpotter® v1 platform (left) and schematic (right) showing the various components that include vector sensors enclosed in flow shields and a Nortek AquaDopp for current velocity measurements (Photo Credit: Frank Spada, Integral)

Table 3: Vector sensor instrumentation and supporting velocity measurements.

Sensor Type	Measurement	Frequency Range	Sensitivity	Calibration Date
M20-040	Acoustic Pressure and 3D particle velocity	50 Hz- 3 kHz	-179 dB re V/ μ Pa (pressure) and 20-80 dB re V/m/s (particle velocity)	July 2022
M20-100	Acoustic Pressure, 3D particle velocity, digital compass	50 Hz- 3 kHz	-179 dB re V/ μ Pa (pressure) and 20-80 dB re V/m/s (particle velocity)	July 2022
Aquadopp Profiler with HR firmware	3D current velocity	3 cm-3 m above seabed	cell size 7-150 mm	February 2023
M20-105	Acoustic pressure and 3D particle velocity	10 Hz - 3 kHz	-176 dB re V/uPa (pressure) and 45 - 80 dB re V/m/s (particle velocity)	July 2022


Figure 5: Previous deployments of NoiseSpotter® (left: v2, right: v1).

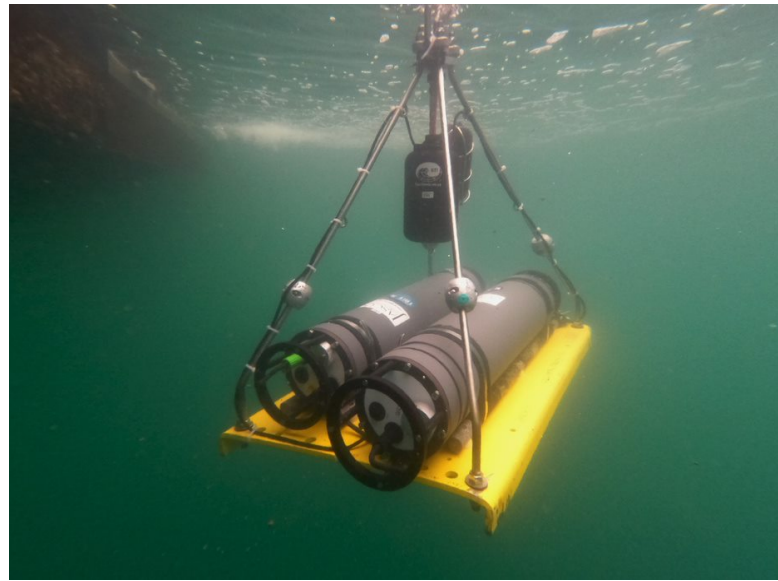


Figure 6: PNNL vector sensor, shown here without flow shield (photo credit: Shanon Dell - PNNL)

7.2.2 PNNL Vector Sensor

The PNNL sensor is an off-the-shelf Geospectrum particle motion sensor (M20-105) that is nearly identical to the sensors integrated with the NoiseSpotter®. The M20-105 is sensitive to acoustic frequencies in the 1-3000 Hz range, with a flat frequency response on the pressure channel and a peak in the response at 600 Hz on the particle velocity channels. Calibration and data units follow the same protocols as the NoiseSpotter®, and the pressure channel has a nominal sensitivity of -176 dB re V/ μ Pa, comparable to the NoiseSpotter® sensors. Before this TEAMER test, the PNNL system was tested on a custom-built frame in a low-current configuration in the quiescent waters of Sequim Bay without a flow shield for 2 days, January 24-26, 2023 (Figure 6). Results from this test showed that the sensor package recorded continuously for the entire deployment period with good data quality. A flow shield similar to the NoiseSpotter® was added to the PNNL sensor package prior to data collection in the tidal channel near the turbine.

7.2.3 DAISYs

A detailed description of the DAISYs can be found in Polagye et al. 2024. Each DAISY is a free-drifting hydrophone system designed to characterize underwater noise around marine energy converters, either individually or in a group to localize sound sources. Two configurations of the DAISYs were deployed at MCRL. Both configurations have a common surface expression equipped with GPS and radio-frequency tracking. Similarly, a common hydrophone package consists of the hydrophone and data logger, pressure sensor, and inertial measurement unit (IMU). The hydrophone package also includes a GPS that acquires pulse-per-second synchronization while at the surface, which is repeated by a precision oscillator when at depth. This supports acoustic localization using groups of DAISYs. The first configuration, shown in Figure 7, is the standard version for measurement in currents. Here, the surface expression is coupled to the hydrophone recording package by a flexible tether, resulting in a hydrophone depth of ~2.5 m. The

pressure-sensitive hydrophone element is enclosed in a fabric flow shield to minimize flow noise. The second configuration is a “shallow” variant, in which the hydrophone package is rigidly coupled to the surface expression and does not incorporate a flow shield (Figure 8). The hydrophone depth for the shallow DAISYs is 1 m. Further details of DAISY sensors incorporated into the surface expression and hydrophone package are presented in Table 5.

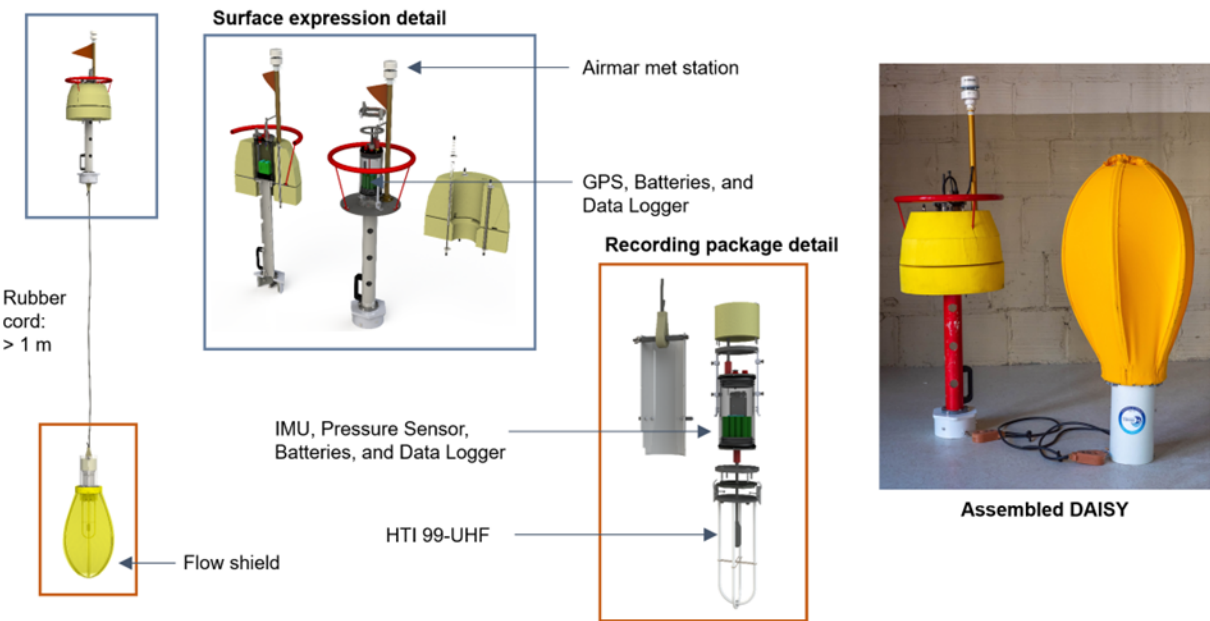


Figure 7: Standard DAISY overview. (left) Rendering of DAISY configuration during deployment in currents. (middle) Exploded views of surface expression and sub-surface hydrophone package enclosed by the flow shield. (right) As-built DAISY configured for testing currents.

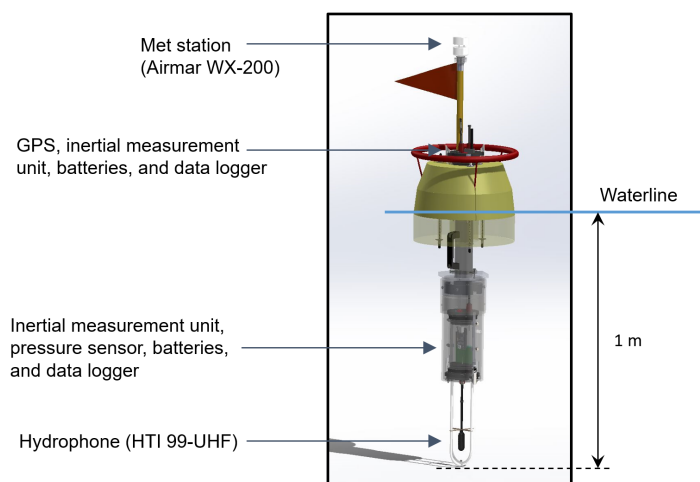


Figure 8: Shallow DAISY overview.

Table 4: DAISY instrumentation

Instrument	Data Streams	Sample Rate [Hz]
Surface Expression		
Global Positioning System (GPS)	Location Speed over ground Direction over ground	>1
Weather Station (Airmar WX200)	Backup GPS Wind speed and direction Air temperature Air pressure	1
Inertial Measurement Unit (IMU)	3-axis accelerometer 3-axis magnetometer 3-axis gyroscope	50
Hydrophone Recording Package		
Hydrophone (HTI 99-UHF)	Acoustic pressure (calibrated May 2021 by PNNL and Ocean Networks Canada)	512,000
IMU	Same as surface	50
Pressure	Depth (estimated from pressure)	5
Backup GPS	Location of deployment and recovery	>1

7.2.4 Turbine Lander

The Turbine Lander contains two sets of instrumentation, both of which communicate with a shore-side computer that logs the data streams (Table 5). The first pertains to turbine operation and performance. The second pertains to environmental measurements. Turbine operation sensors include measurements of electrical power at the generator terminals, rotation rate, and operating state. Currents are measured by an acoustic Doppler current profiler (Nortek Signature 1000) on the lander platform on a leg perpendicular to the dominant current direction. The environmental sensing package (Lander Adaptable Monitoring Package - LAMP) includes:

- Stereo optical cameras with artificial lighting
- Two BlueView sonars (M900-2250)
- Tritech sonar (Gemini 720is)

- Four-element passive acoustic array (HTI 99-UHF with custom data acquisition similar to the DAISYs)

Data acquisition for the environmental sensors can be continuous (which generates extremely large volumes of data), occur on a fixed duty cycle, or observe continuously, but only archive data when certain conditions are satisfied (e.g., a target of interest is detected in a sonar data stream). The sonars and cameras are mounted to the rotator head (Figure 2) and oriented towards the turbine to monitor for fish interactions with the rotor. The hydrophone array is not shielded from the currents and, consequently, propagating sound from the turbine and other sources are periodically masked by flow noise. While the data streams from the LAMP may be helpful to correlate fish presence/absence with turbine operating state and exposure to particle velocity, that analysis is beyond the scope of this project.

Table 5: Turbine Lander instrumentation relevant to acoustic characterization

Measurement	Source	Sample Rate
Rotation rate	24 bit absolute encoder with (Siemens AS24DQI) with +/- 40" angular error	250 Hz
Electrical power at generator	Transducer integrated into generator	250 Hz
Turbine operating state	Command input	250 Hz
Inflow velocity	Nortek Signature 1000	4 Hz samples 10-second smoothed average used for rotor control update (subject to change based on measurements)
Acoustic pressure	4-element hydrophone array	Minimum 50 kHz/channel

7.3 Test and Analysis Matrix and Schedule

A 14-day measurement period was proposed in the test plan, but due to the loss of NoiseSpotter®v1, deployments were conducted asynchronously over the course of several months, as detailed in Table 6. The PNNL sensor and NoiseSpotter®v1 were concurrently deployed for a one-day period on day 1. Tidal currents did not exceed the turbine cut-in speed during this deployment (no turbine power generation), so the turbine was motored for a 5-minute period to provide a sound source for data evaluation. The following day, the PNNL sensor and NoiseSpotter®v1 were recovered and redeployed as planned, though only the PNNL sensor was recovered from this deployment. DAISY surveys were conducted during two days while both vector sensor systems were deployed. At this time, the project team was unaware that NoiseSpotter®v1 had been lost, so DAISY drifts targeted the NoiseSpotter®v1 deployment location. Finally, NoiseSpotter®v2 was deployed 3 months later in February, 2025.

Table 6: Survey schedule, by day

Day	Nov 6	Nov 7	Nov 8	...	Nov 15	Nov 16	Nov 17	...	Feb 1	...	Feb 14
Mobilization											
Benchmarking Deployment											
PNNL sensor deployment											
NoiseSpotter® v1 Deployment											
Noisespotter® v2 Deployment											
DAISY Surveys											

7.4 Safety

All project team members participating in field operations participated in all relevant PNNL-led safety trainings and followed PNNL safety protocols while working on research vessels.

The PNNL dive team supported deployment and recovery of the NoiseSpotter® and PNNL sensor by placing screw anchors to secure the platforms at deployment, then removing screw anchors and attaching a recovery line at recovery. All operations were conducted around slack tide to avoid unsafe operating conditions due to strong currents. This procedure is routine for the PNNL dive/vessel crew and has been performed safely multiple times in the past.

The primary personnel risk during DAISY deployment and recovery is entanglement with the cord that connects the surface expression to the hydrophone package. To mitigate risk, two personnel deployed each DAISY, not releasing the systems until all cordage was visually confirmed to be free of obstruction or entanglement risk. A secondary personnel risk is falling overboard during DAISY deployment or recovery. This risk was mitigated by:

- (1) the choice of vessel: low freeboard reduces the need to lean over the side to deploy or recover DAISYs; high maneuverability facilitates recovery;
- (2) survey design: deployment and recovery are conducted while drifting with the currents, which minimized relative velocities; and
- (3) DAISY design: large “grab rings” and handles facilitate deployment and recovery of the surface expression using boat hooks.

For all vessel operations, any member of the team was encouraged to call an “all stop” if they observed an imminent safety risk or were unsure of next steps. Vessel operations did not commence if weather conditions present unsafe working conditions due to wind/waves, air temperature, or precipitation. Due to the timing of the tidal currents, DAISY operations took place after dark, which heightened safety considerations due to limited visibility in the event of a person falling overboard.

7.5 Contingency Plans

Success of this test was contingent on deployment of the Turbine Lander in Sequim Bay. If the Turbine Lander deployment had not occurred, this test would not have been conducted.

Both the NoiseSpotter® and PNNL sensor were bench tested on Day 0 to ensure data were being collected. Battery output was checked to verify a full charge, and the hard drives were erased to ensure the availability of adequate storage for the deployment duration. If issues had been identified with recorded data, the schedule would have been adjusted to allow for sensor assessment or repair. If issues had been identified with the hard drive or battery, spares would have been utilized.

Our contingency plan did not account for complete platform loss sensor loss, which did occur. Lessons learned and recommendations for future tests are discussed in Section 8.2.

7.6 Data Management, Processing, and Analysis

7.6.1 Acoustic Vector Sensors

Given the absence of specific standards for the processing of vector sensor data, and in particular the directional processing of vector sensor data, best practices learned from experience as well as new techniques developed for this dataset were applied to vector sensor data processing.

Each vector sensor produces four sets of voltages that represent the pressure and particle velocity measurements in three directions (x, y, and z). Each pressure channel was converted to a voltage spectrum [V/Hz] using a Fast Fourier Transform (FFT) with user selectable FFT length (typically 4096 points with no overlap across segments and Hamming window applied prior to FFT, giving a frequency resolution of 4.88 Hz (NoiseSpotter® v1, sampling frequency 20 kHz), 2.34 Hz (NoiseSpotter® v2, sampling frequency 9600 Hz), and 1.95 Hz (PNNL vector sensor, sampling frequency 8000 Hz). Frequency-dependent, sensor-specific, receive voltage sensitivity were applied to convert this to a complex pressure spectrum [$\mu\text{Pa}/\text{Hz}$] over the sensor measurement range of (50 Hz to 3 kHz for the NoiseSpotter® v1, 10 Hz to 3 kHz for NoiseSpotter® v2), and 10 Hz to 3 kHz for the PNNL sensor). A similar procedure was implemented on the raw voltages that represent particle velocity measurements, where frequency-dependent, sensor-specific, receive voltage sensitivity were applied to convert these to complex velocity spectra [$(\text{m/s})/\text{Hz}$]. The final calibration step was the application of a sensor- and frequency-dependent phase shift (relative to the pressure channels) to each velocity spectrum. The start time of each frequency-calibrated spectrum and the two-sided spectrum were written to MATLAB binary files for further processing. Filenames contain the start time of the respective data segment.

Following the Day 1 deployment to benchmark NoiseSpotter® v1 and PNNL vector sensor measurements, data were offloaded and examined. Data were calibrated using sensor-specific calibration curves for pressure, particle velocity and the phase offset between pressure and particle velocity. Data quality (expected source and ambient noise levels) was examined to ensure data integrity. Data quantity was verified to ensure no gaps are present. Data were backed up to ensure no data loss due to hard drive failure.

Time- and frequency-resolved directional processing provided the team with an evolution of tidal turbine sounds over the measurement period. ‘Azigrams’ were calculated from the vector sensor data

using the methods discussed in Thode et al. 2019, where pressure-velocity cross-spectra are utilized to provide time- and frequency- evolving azimuthal and elevation angles. An example of an azigram computed on NoiseSpotter® v1 data gathered near the CalWave WEC is shown in Figure 9, with sounds associated with the WEC demarcated by the yellow boxes. Sound pressure and particle motion data were also used to calculate the time- and frequency-resolved normalized transport velocity (NTV). The NTV is dimensionless and ranges from 0 to 1, with a value of 1 indicating that most of the acoustic energy in that time/frequency bin is from a single bearing, and a value of 0 indicating that acoustic energy is equally distributed from all bearings (Tenorio-Hallé et al. 2022). Therefore, sound from a distinct source (e.g., the turbine) will have higher NTV values than ambient noise or flow noise.

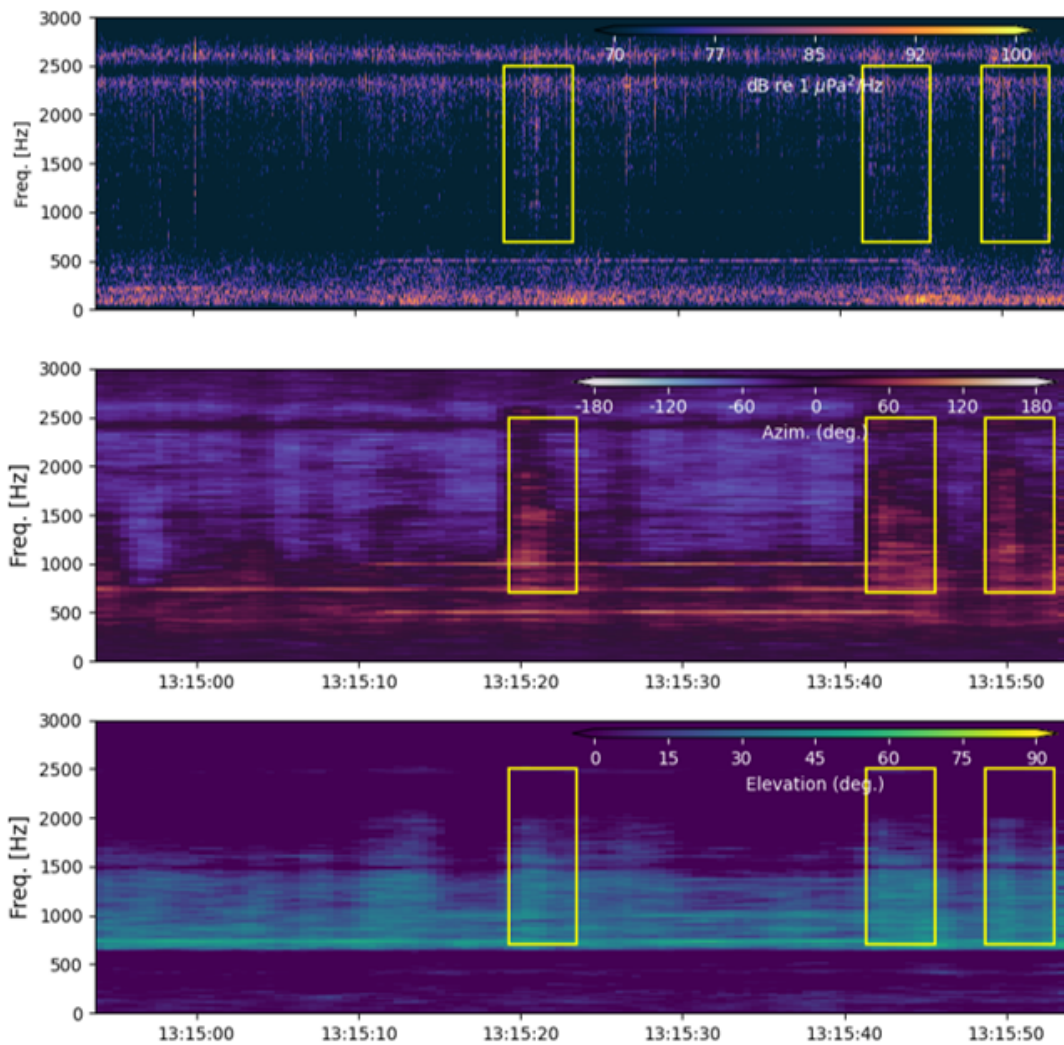


Figure 9: Example of directional processing of NoiseSpotter® data gathered near a wave energy converter, along with automated directional characterization (yellow boxes) of sound attributed to the WEC.

7.6.2 Drifting Hydrophones

DAISY acoustic data were processed according to IEC technical standard 62600-40 (2019). The voltage produced by the hydrophone was converted to a voltage spectral density [dB re 1 V²/Hz] using a Discrete Fourier Transform with 1-second windows and 50% overlap. Frequency-dependent receive voltage sensitivities from prior calibration were applied to convert this to pressure spectral density [dB re 1 μ Pa²/Hz] over a frequency range of 0.001 – 200 kHz. To reduce file size, the 1 Hz spectral density was averaged across millidecade bands (Martin et al. 2021) for frequencies greater than 434 Hz (the point at which millidecade frequency bands are > 1 Hz). This results in a mild loss of fidelity at higher frequencies, but reduces file sizes by an order of magnitude. Uncertainty in acoustic spectra associated with temporal variability was quantified by the interquartile range as a function of frequency.

Co-temporal data from other sensors (e.g., depth) are embedded with the acoustic data, providing georeferenced location and environmental covariates (e.g., wind speed, DAISY speed over ground). Raw data QA involved:

1. A review of metadata time series to identify metadata sensor malfunctions or hydrophone impairment (e.g., irregular depth, significant tilt angle);
2. A review of the bivariate pressure spectral density (i.e., probability of a given spectral density as a function of frequency) to identify changes in the instrument noise floor and variations in pressure spectral density within a single drift;
3. Review of each drift using acoustic playback synchronized with a spectrogram (pressure spectral density as a function of time) to identify masking ambient noise (anthropogenic or natural) and DAISY self-noise. The review tool allows periods with high levels of ambient noise or self-noise to be flagged and excluded from further analysis; and
4. Review of groups of drifts to identify any clock issues (e.g., file time stamp error) based on approximate time of arrival for common, high-amplitude signals (e.g., deployment vessel engine restart).

Processed data from three or more co-temporal drifts can be used to localize sound sources using time delay of arrival (TDOA). The first step in TDOA processing is to identify the arrival time and frequency ranges corresponding to events of interest in each of the co-temporal DAISY tracks. These events are manually identified during the data review process. For each event, we apply a bandpass filter to suppress noise outside of the band of interest and then apply a Hilbert transform. In each event time series, the index of the maximum absolute value of the cross-correlation is taken as the reference time of arrival. When using the same portions of the time series on all DAISYs, the indices associated with the peak in the cross-correlation corresponds to the time delay between the signals, albeit with uncertainty introduced by the propagation environment and DAISY position. With these arrival times, we apply a TDOA localization method (Wahlberg et al. 2001) to estimate the origin of the event. This is most effective when the signal-to-noise ratio for the event is relatively high, the source is located within the polygon formed by the group of DAISYs, and multiple DAISYs are not in line with the source.

7.6.3 *Turbine Lander*

Given the relatively high data rates for Turbine Lander sensors (Table 5), performance measurements were smoothed into 1-minute averages for visualization.

7.7 **Data Analysis**

Particle motion and sound pressure data gathered over the measurement period were processed and reported with the goals of characterizing the acoustic environment during the operation of the Turbine Lander and relating measured acoustic data to turbine operating modes.

The team implemented ‘first-order’ standard acoustic data analysis products such as long-term spectral and azimuthal averages (LTSA), and event specific power spectral densities. The result of these analyses was a characterization of the acoustic environment during the deployment of the tidal turbine, or any other logged activities during the deployment.

Directional processing was used to relate to known turbine operating modes to sounds from the turbine. Data analysis operations are described below, as they pertain to the specific project goals.

7.7.1 *Benchmark the new acoustic particle motion capability at the PNNL TEAMER facility*

Calibrated data gathered during the Day 1 concurrent system test were compared between the PNNL vector sensor and the NoiseSpotter. An initial comparison of LTSA data between the two sensor packages was used to fine-tune PNNL data processing and calibration codes. Consistency of directional estimates was verified by comparing snippets of azimuthal angles processed using each system’s particle velocity data for turbine sound and the sound from the PNNL water intake pump, which produced a continuous tone at approximately 160 Hz.

7.7.2 *Quantifying sound generated by the turbine and identifying the sources of generated sound*

Spectrograms, azigrams, and NTV were calculated for all recorded vector sensor data, and periods contaminated by boat noise were manually removed from the dataset. While azigrams contain valuable information about the directional origin of recorded sound, they are relatively noisy and processing long periods of data to identify sounds from the direction of the turbine in a long recording is not straightforward. We developed a new approach to visualize sound that might be attributed to the turbine using a binary mask calculated using the power spectral density, the azigram, and the NTV. Sounds that might be attributed to the turbine can be identified using a combination of these three metrics if they:

- have sound pressure amplitude above background levels (i.e., spectrogram exceeds a specified threshold),
- have a bearing in the direction of the turbine from the vector sensor (i.e., azigram falls in a specified range),

- and have a NTV value near 1.

Therefore, thresholds can be applied to these three metrics to create a binary mask indicating times and acoustic frequencies that might contain turbine-attributable sounds. An example of this using data recorded by the PNNL vector sensor during the one-day benchmarking deployment is shown in Figure 10.

While the binary mask presents a clear representation of the sound that might be attributed to the turbine over a short period, identification of all potential turbine sounds over an extended time period would require rigorous human scrutiny of the data. To speed analysis, the binary mask for each one-minute time window was summed along the frequency axis to create a “long-term histogram” that indicates the fraction of time/frequency bins in each time window that could be attributed to the turbine.

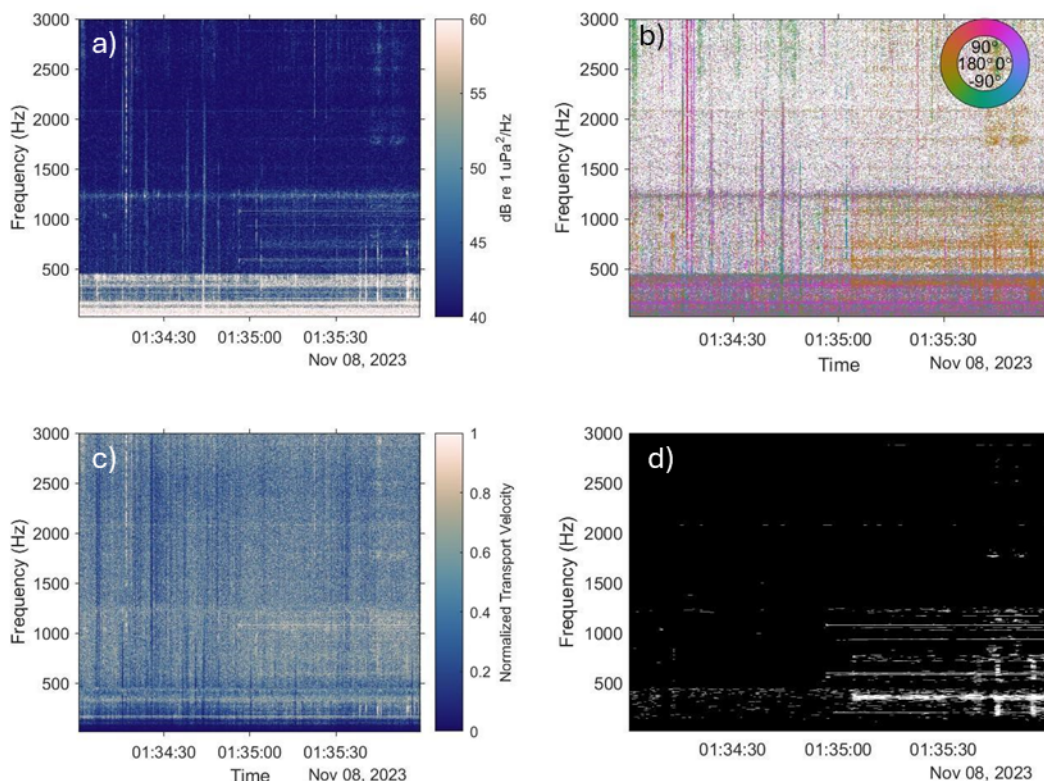


Figure 10: Spectrogram (a), azigram (b), normalized transport velocity (c), and binary mask (d) from the PNNL sensor for a two minute period when the turbine was motored. The turbine starts up at approximately 1:35:05, and is located at a bearing of approximately 180 degrees from the vector sensor. The constant tones at approximately 160 and 320 Hz are from a nearby water pump, which was located at a bearing of approximately 90 degrees from the turbine.

7.7.3 Broaden the general understanding of radiated noise from marine energy converters

Data gathered by the NoiseSpotter® and the PNNL vector sensor provide the first measurements of particle motion from a tidal current turbine. This analysis not only provides insight into propagation characteristics of turbine sound, but also informs future measurement to monitor underwater sound from turbines.

7.7.4 Compare acoustic measurement methods

Far from reflecting boundaries, pressure and particle velocity are directly related by the acoustic impedance of sea water. The relationship is not as straightforward close to reflecting boundaries such as the sea floor, requiring separate measurements of the two quantities. Particle velocity computed from pressure is compared to the direct measurements of particle velocity to yield insights into the deviations between the two quantities, which can inform future propagation modeling efforts.

8 PROJECT OUTCOMES

8.1 Results

8.1.1 Vector Sensor Benchmarking

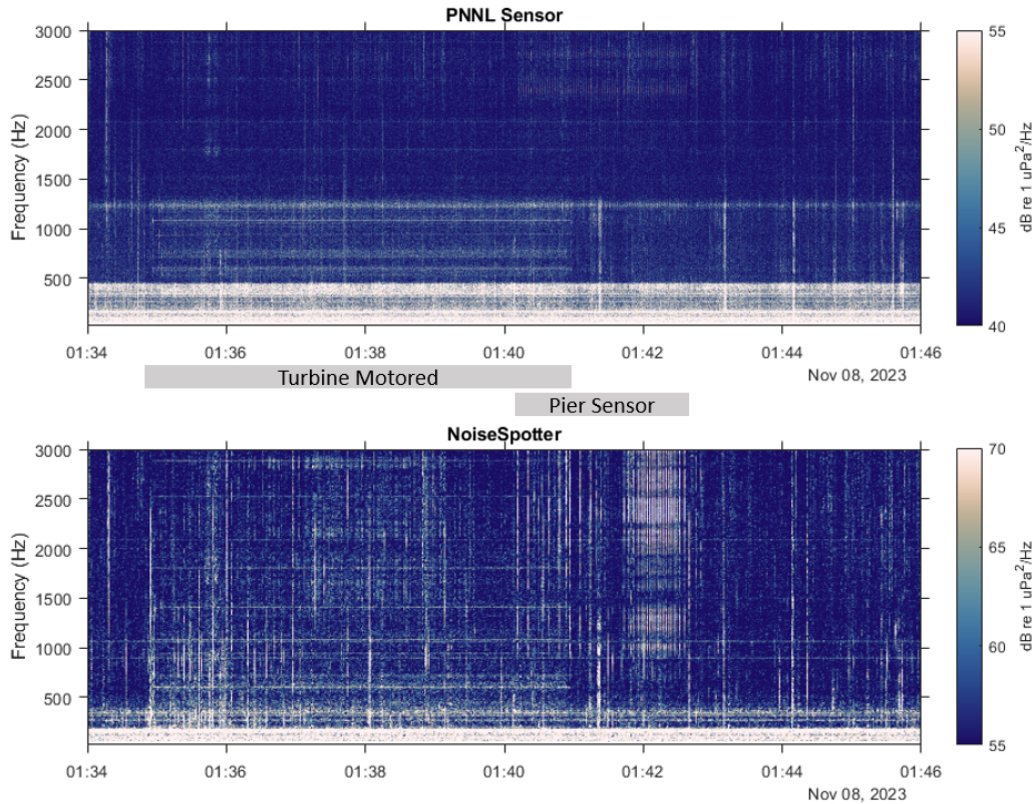


Figure 11: Spectrograms from the PNNL sensor (top) and NoiseSpotter® v1 during an 8-minute period during the benchmarking deployment when the turbine was motored.

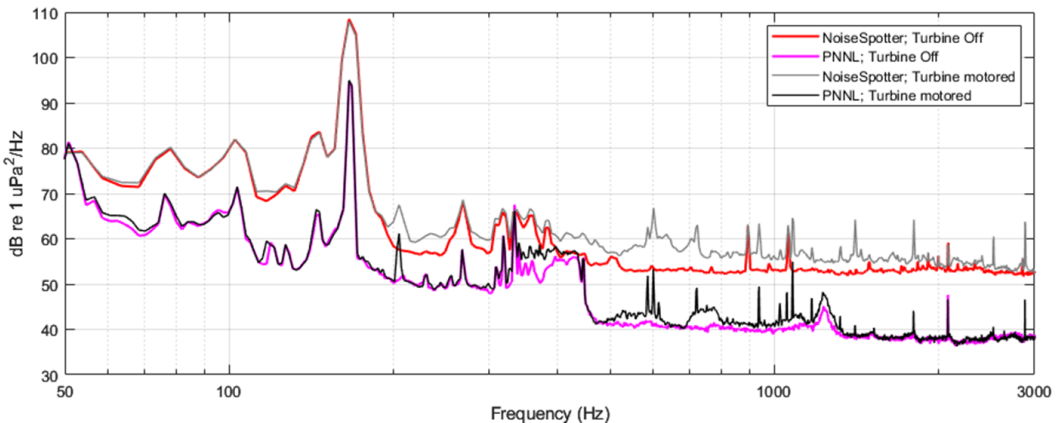


Figure 12: Median power spectra from the PNNL sensor and NoiseSpotter® during periods when the turbine was off and when the turbine was motored during the benchmarking deployment.

Figure 11 shows spectrograms from the PNNL sensor and NoiseSpotter®v1 for an 8-minute period when the turbine was motored during the first day of data collection. There was an approximately 20 second time lag between the two sensors due to lack of synchronization that was manually identified through common sounds and corrected. Both sensors detected tones associated with the turbine turning on, though, as subsequently discussed, amplitudes differ between the sensors. An unrelated sensor on the PNNL research pier began pinging for three minutes at the end of the period when the turbine was operated, and was also detected by both vector sensors, but more evident in the NoiseSpotter® v1 spectrogram.

Figure 12 compares the median spectra recorded by the PNNL sensor and NoiseSpotter®v1 for a two-minute period when the turbine was off (Nov 8 1:44-1:46 UTC) and a two-minute period when the turbine was motored (Nov 8 1:36-1:38 UTC). Several observations can be made. First, there is an approximately 15 dB difference in amplitude between the two sensors. Further, there is a notable cut-off in amplitude above 400 Hz in the data from the PNNL sensor. This cut-off gradually increased in frequency and decreased in amplitude over the course of the deployment, and was observed in the subsequent deployment as well. While more conclusive testing is required, we hypothesize that the flow shield trapped an air bubble inside, which attenuated higher frequencies and slowly dissipated over the course of the deployment. Despite these differences in amplitude, the same tonal structure is generally observed by both sensors. The highest amplitude tone at 160 Hz is from the PNNL seawater intake pump, and was constant throughout the deployment except for a short period when it was shut off during DAISY surveys. Higher frequency tones associated with the turbine are observed around 200 Hz, 500 Hz, 600 Hz, 900 Hz, and above 1000 Hz. Notably, two tones at 900 and 1100 Hz were recorded by the NoiseSpotter® v1 while the turbine was off and while it was being motored, but were not recorded by the PNNL sensor. Unfortunately, the loss of NoiseSpotter® v1 prevents us from further exploring these differences, and because NoiseSpotter® v2, which had a new datalogger and new sensors, was used for subsequent measurements, this comparison is not particularly informative for interpretation of the subsequent results presented in this report. However, comparison between sound pressure levels measured by the PNNL sensor and the DAISYs, discussed in Section 8.1.5, provided an additional opportunity to benchmark PNNL sensor measurements.

8.1.2 Vector Sensor Measurements of Turbine Operational Noise

First, we analyzed periods when the turbine started up (i.e., flow speed reached turbine cut-in speed) to determine whether sound from the turbine could be detected. Figure 13 shows a spectrogram and azigram recorded by the PNNL sensor during turbine startup on November 11, along with the concurrent recording of turbine rotational rate (RPM). The sound from the turbine is faint (<60 dB re 1 $\mu\text{Pa}^2/\text{Hz}$), but a clear signal is detected when the turbine starts in both the spectrogram and azigram. The 160 Hz tone and harmonics from the water intake pump are at an angle of approximately 90 degrees from the turbine. Notably, manual inspection of the spectrograms and azigrams also revealed that the sound from mechanical wipers used for the LAMP optical cameras was also detected during slack tides (Figure 14). The wipers were actuated once every 30 minutes, which aligns with the recorded acoustic signal.

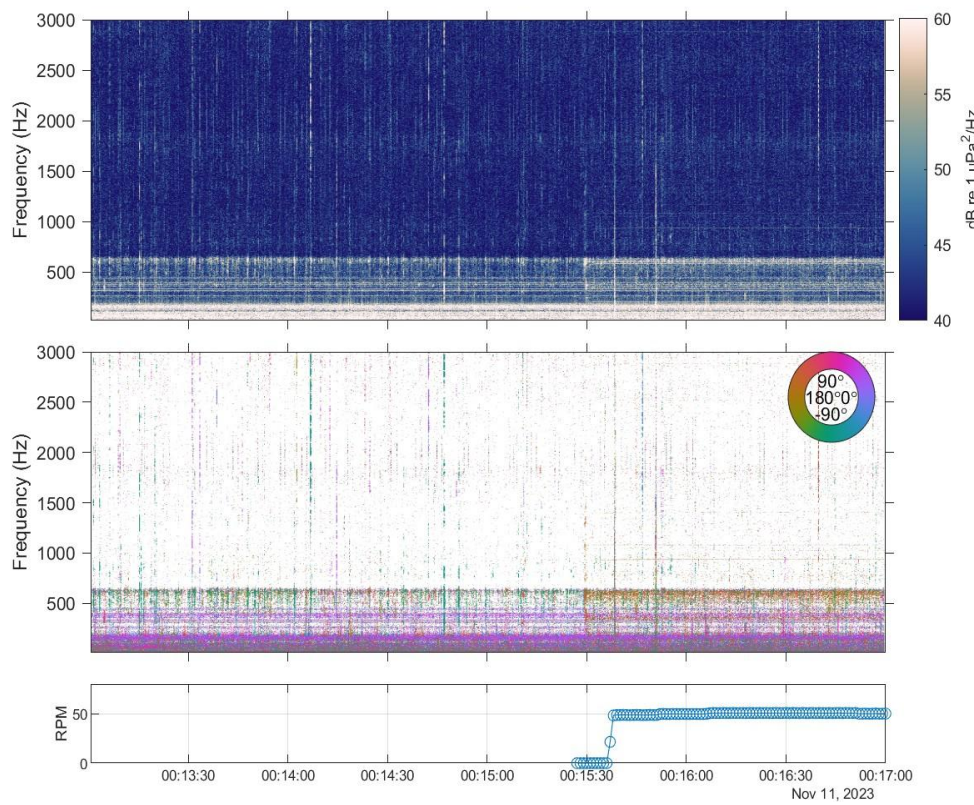


Figure 13: Spectrogram (top) and azigram (middle) recorded during a period when the turbine started up during normal operation. Turbine rotation rate (RPM) is shown in the bottom panel.

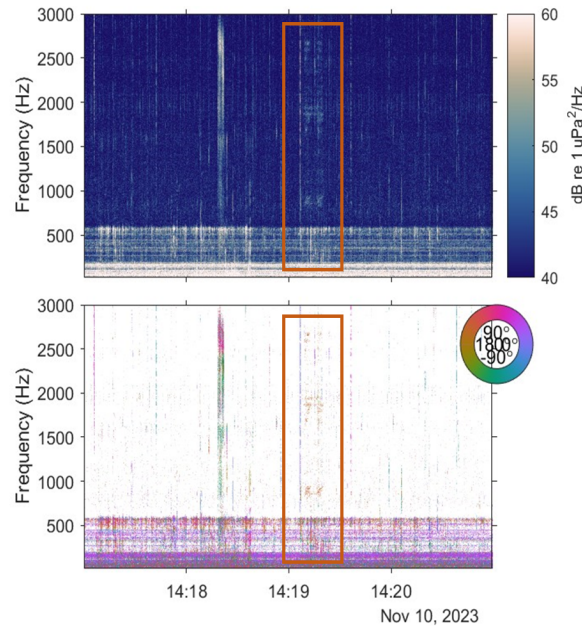


Figure 14: Spectrogram (top) and azigram (bottom) recorded by the PNNL sensor showing the sound from camera wiper actuation.

After confirming that turbine sound was detected, we analyzed changes in turbine sound with turbine operational state. To do this, we removed periods contaminated by boat noise and binned pressure spectra by turbine rotational rate (10 RPM bins) and calculated the median pressure spectral density for each bin. Results for one tidal cycle during the PNNL sensor deployment (November 15-16) are shown in Figure 15, and results for one tidal cycle during the NoiseSpotter® v2 deployment are shown in Figure 16.

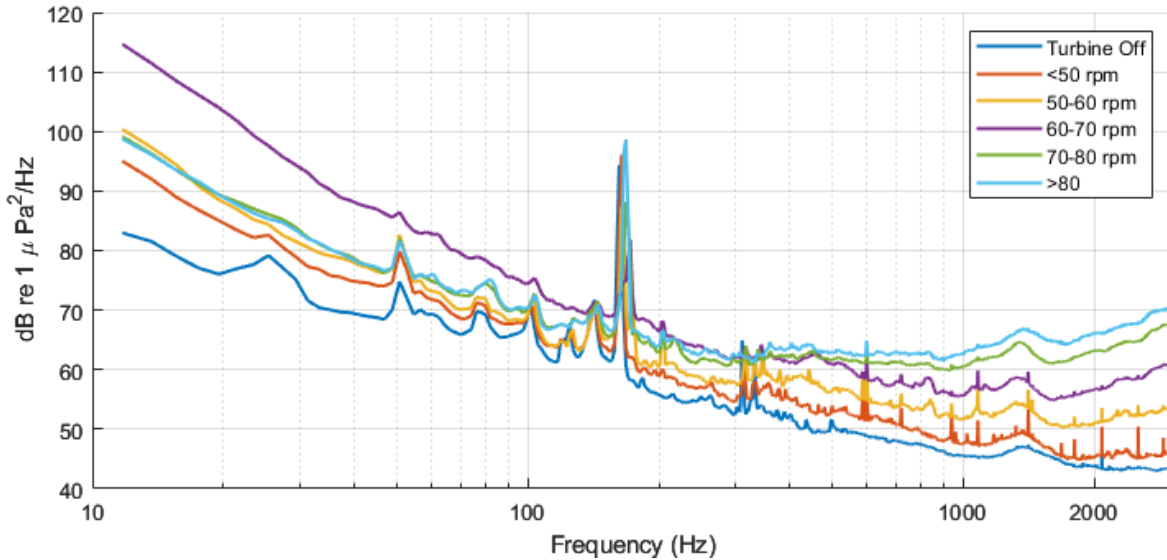


Figure 15: Median pressure spectral density binned by turbine rotation rate, recorded by the PNNL sensor on November 15-16.

Several observations can be made. First, while the flow shield likely reduced flow noise contamination, flow noise is still observed below 100 Hz in data from the PNNL sensor. However, flow noise contamination decreases during peak rotation rate (peak flow rate), which is counterintuitive since turbine rotation rate increased linearly with flow rate (turbine inflow velocity). This is most likely a consequence of spatial heterogeneity of flow conditions in the channel (i.e., peak flow speeds at the turbine location do not correlate with peak flow speeds at the vector sensor location). The 160 Hz tone associated with the water intake pump is observed during all turbine states. Tones associated with turbine operation are observed, though at higher rotation rates/flow speeds it is difficult to disassociate turbine sound from increases in ambient noise. Increasing ambient noise with increasing flow speeds due to sediment transport has been observed in other passive acoustic datasets recorded in tidal channels in Puget Sound (Bassett et al. 2014; Cotter et al. 2024).

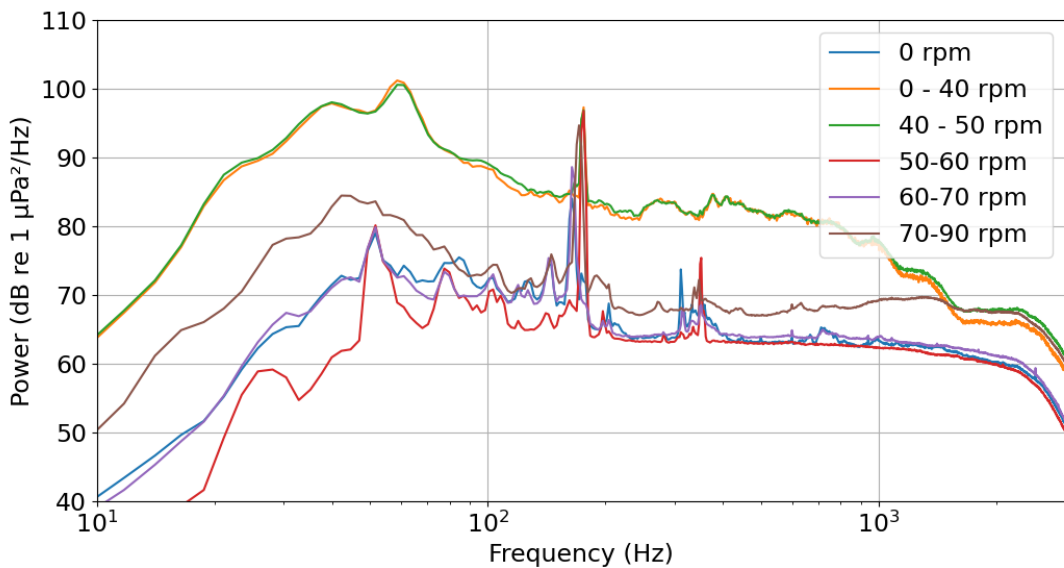


Figure 16: Median pressure spectral density, binned by turbine rotation rate, recorded by the NoiseSpotter® v2.

NoiseSpotter® v2 measurements during a single tidal cycle in February (initially after one tidal turbine blade was damaged and lost) shows generally greatest acoustic energy (Figure 16), when rotation rates are less than 50 RPM. While a tonal structure appears above 50 RPM, specific coherent tones are difficult to isolate, with the exception of the tone at approximately 600 Hz, which is consistent with that observed during turbine motoring on November 7 (Figure 12). Changes in the turbine acoustic signature (i.e., faint tones are no longer detectable) between the PNNL sensor deployment and the NoiseSpotter® v2 deployment might be attributed to the lost blade, biofouling on the turbine structure, or degradation/wear in the turbine bearing pack.

The long-term histogram and long-term spectral average offer more insight into how the turbine acoustic signature evolves over a tidal cycle. Figure 17 shows the long-term histogram, long-term spectral average, and turbine rotation rate for a representative tidal cycle during the PNNL sensor deployment (selected due to minimal contamination from passing boats). A 1-minute time window was used for both the long-term spectral average and histogram, and minutes containing vessel noise have been manually removed from the dataset. The long-term histogram provides an estimate of the percentage of sound in each time/frequency bin that is coming from the turbine direction. While increased sound levels during the tidal exchange are clear in the long-term spectral average, frequency structure of sound from the turbine is only clear in the histogram. Generally speaking, there is more acoustic energy measured from the turbine on the ebb tide, which is likely related to higher flow speeds, and therefore higher rotation rate, on ebb tides. The histogram also shows less acoustic energy from the turbine direction during peak tides/turbine rotation rate; however, this is likely attributed to increased ambient noise (more sound from all directions). The histogram also indicates that there was a faint tone at approximately 2 kHz from the turbine direction that started before turbine startup and persists after turbine shutdown. The source of this tone has not been identified.

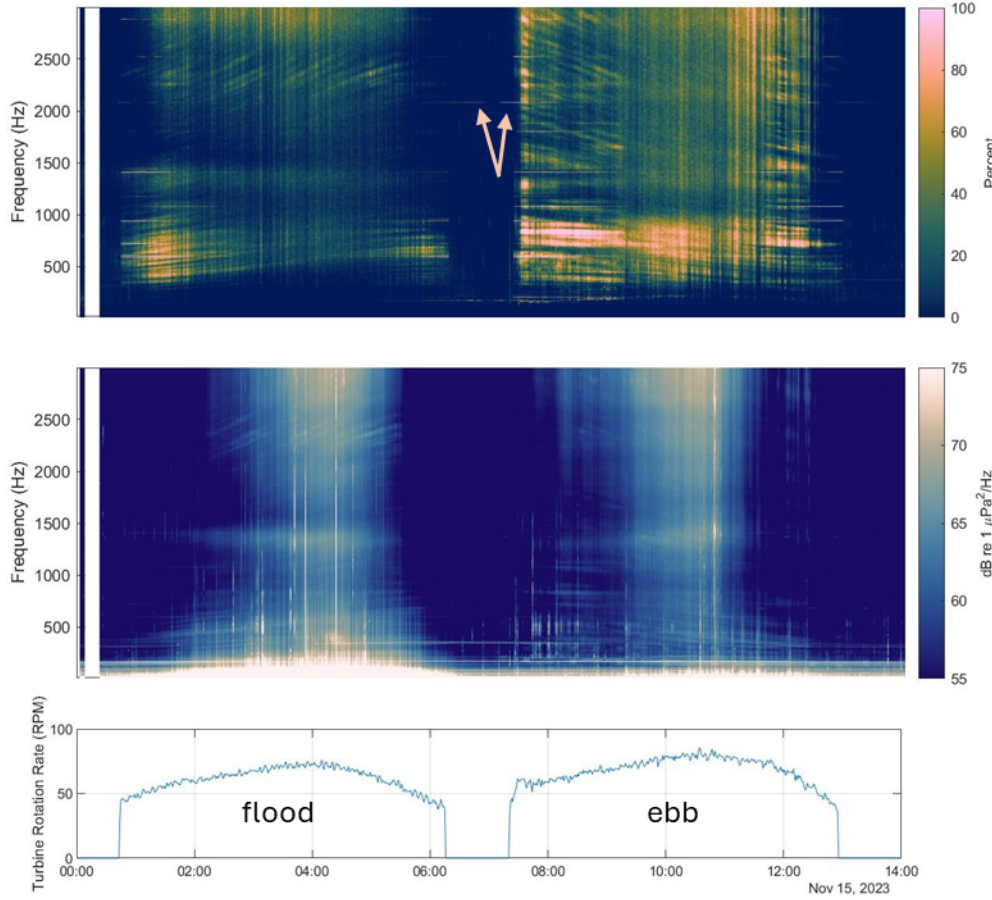


Figure 17: Long term histogram (top), spectrogram (middle) and turbine rotation rate (bottom) for a representative tidal cycle, recorded by the PNNL sensor. Arrows on the long term histogram indicate the 2 kHz tone that persisted before/after turbine startup/shutdown.

Figure 18 shows a long-term spectrogram and long-term azigram from the NoiseSpotter® v2 measurements over multiple days in February 2024, after one turbine blade was damaged. The true bearing of the turbine relative to the NoiseSpotter® v2 was 90 degrees to the east, and a regular pattern of increased acoustic activity at that bearing is observed that coincides with turbine operation and increases with rotation rate. Similar to the PNNL data from November, there is a more prominent acoustic signature during the ebb tide.

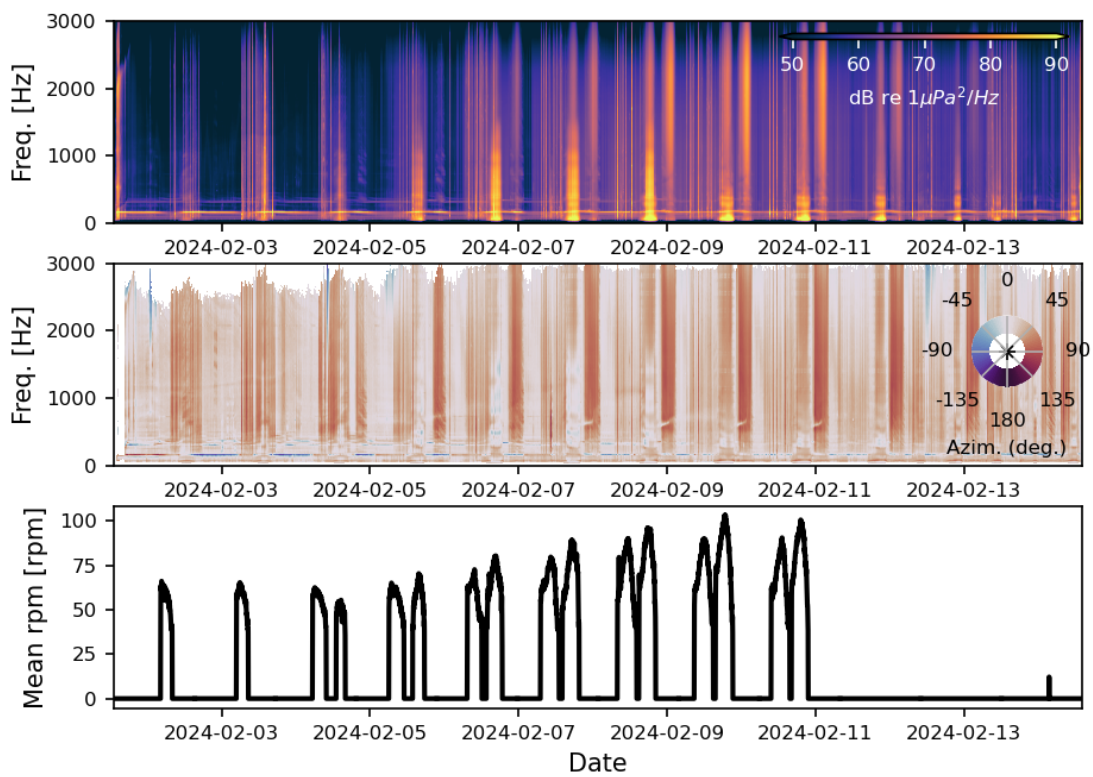


Figure 18: Long-term spectrogram (top), long-term azigram (middle), and turbine rotation rate (bottom) during the NoiseSpotter® v2 deployment.

A closer look at turbine activity spanning 14 hours (approximately a single flood-ebb tidal cycle) is shown in Figure 19, which shows the pressure spectrogram, azigram, long-term histogram, and the turbine rotation rate.

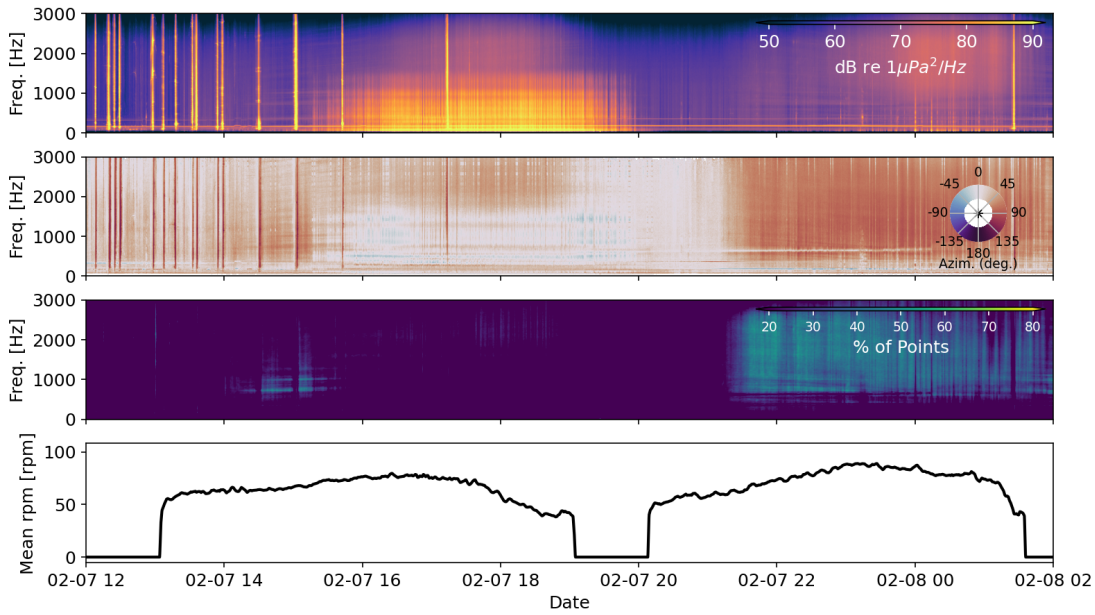


Figure 19: From top to bottom, spectrogram, azigram, long-term histogram, and turbine rotation rate for a single tidal cycle during the NoiseSpotter® v2 deployment.

The spectrogram masked by turbine sounds is computed using the histogram method used in the PNNL vector sensor processing. Once the histogram is applied at each time and frequency bin in the azigram, turbine sounds that have a high frequency of occurrence (>50%) are seen to mostly consist of both mostly longer-duration broadband noise on the ebb tide with very few occurrences on the flood tide. Generally, similar to that observed by PNNL in November, there is increased acoustic energy on the ebb tide relative to flood, likely due to higher rotation rates on the ebb tide. The downward frequency sweeps during the ebb phase are also present in the February data, though not as prominent as during the November deployment. Assuming that these are related to rotor activity, the missing blade in February could be the reason for the less prominent frequency sweeps.

8.1.3 Comparison of measurement methods

When sound propagation can be approximated as a spherical wave, the magnitude of particle velocity, v , can be calculated directly from sound pressure as:

$$v = \frac{p}{\rho * c},$$

Where p is the sound pressure, in Pa, ρ is the density of the water, in kg m^{-3} , and c is the speed of sound in the water, in m s^{-1} . However, in shallow and bathymetrically complex areas, this relationship can be off by up to 6 dB (Dahl et al. 2024). Because measurements of particle motion are important for understanding perception by fish and sound pressure sensors (hydrophones) are cheaper, easier to use, and more readily available than vector sensors, we compared direct measurements of particle velocity to

values calculated from sound pressure. We compared ambient particle motion levels measured during slack tide to minimize the effects of flow noise or platform motion on the comparison.

Figure 20 shows measured and calculated particle velocity as a function of frequency for a five-minute period on November 16, gathered on the PNNL vector sensor, and Figure 21 shows the mean spectra during this period. Generally, the two agree within a few dB above 100 Hz, with the exception of the cut-off in the sound pressure data attributed to air trapped in the flow shield, which was near 1500 Hz at this point in the deployment. Below 100 Hz, the measured particle velocity is higher than calculated values by nearly 20 dB. This could be explained by higher sensitivity of the particle motion sensor (accelerometer) to low frequencies or could be attributed to the fact that these frequencies may be below the waveguide cutoff frequency for the site.

Comparisons between multiple spectral statistics for the measured velocity magnitude and that inferred from pressure over 10 minutes of an ebb flow on February 7 from 14:20 to 14:30 PT for the NoiseSpotter® v2 data are shown in Figure 22. Excellent comparison is seen in the median statistic for inferred (from pressure) and measured velocity magnitude. However, there are significant differences in the outliers (99% and max statistics) that approach 20 dB at frequencies above 100 Hz. These outliers appear to consist of multiple harmonics of a 100 Hz signal that is more pronounced in acoustic pressure than particle velocity suggesting the presence of standing waves in the water column, perhaps from nearby boat traffic.

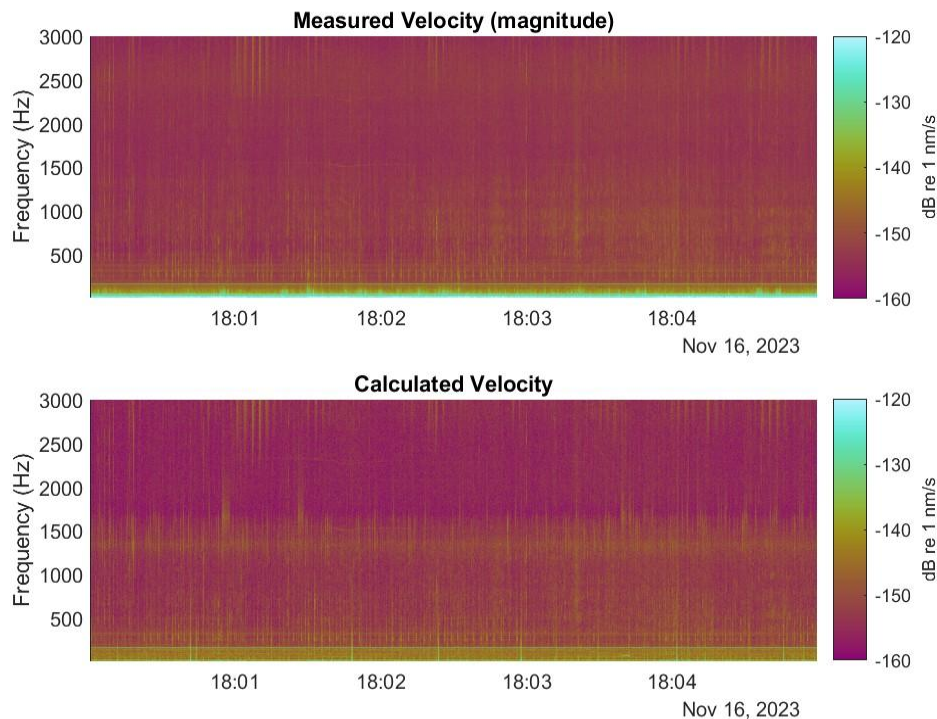


Figure 20: Spectrogram showing sound particle velocity (top), and spectrogram showing sound particle velocity calculated from sound pressure (bottom) measured by the PNNL vector sensor during a 5-minute period during slack tide.

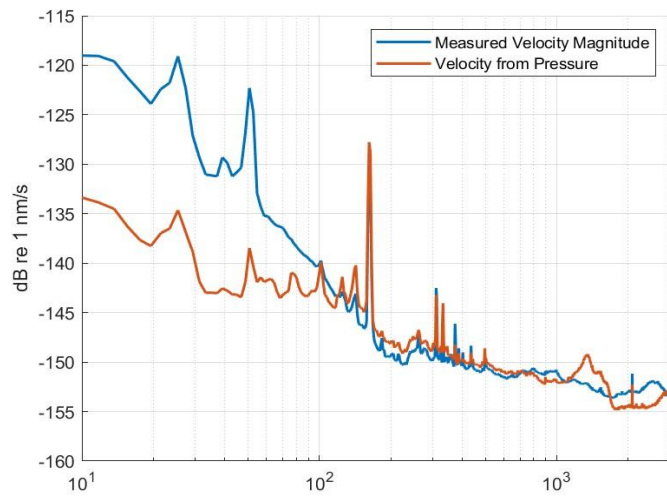


Figure 21: Mean spectra of measured and calculated particle velocity for the same time period shown in Figure 21.

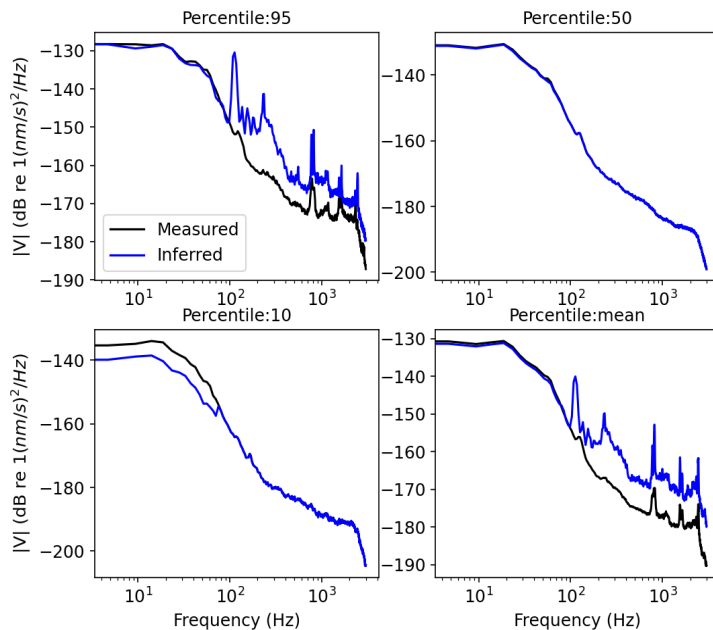


Figure 22: Statistics of measured particle velocity versus those inferred from acoustic pressure. The median (50 percentile) shows excellent agreement between the two. The lower percentiles are affected by flow noise at the lower frequencies (i.e. abnormally high measured particle velocity) while the higher percentiles are affected by outliers when there is higher acoustic pressure relative to particle velocity.

8.1.4 DAISY Survey

As previously discussed, DAISY measurements were conducted on November 15 and 16. Due to the timing of the currents, these were conducted after dark, from approximately 1800 – 2100 local time. The noise signature from the Turbine Lander was most apparent at ranges within 10 m and consisted of:

- tones attributable to the servomotor generator and its variable frequency drive at 4 kHz and 8 kHz;
- “squeaks” attributable to the bearing pack between 1.7 and 2.7 kHz;
- semi-impulsive once-per-revolution “clicks” attributable to the bearing pack between 0.2 and 0.6 kHz;
- metallic “clanks” between 1.6 and 3 kHz, likely associated with gravel or cobble impacts on the foundation (these were observed when surface currents exceeded 1.6 m/s); and
- tones attributable to the bearing pack that varied with rotation rate.

In dockside tests, the highest intensity variable-frequency tone (f_{peak}) was found to vary linearly with rotation rate as

$$f_{peak} = 2.8109\omega - 1.1091$$

where ω is the turbine rotation rate in RPM. Depending on the rotation rate, other tones of lower intensity were also observed.

Spectrograms and an associated periodogram around the closest point of approach for a DAISY drift are shown in Figure 23. During this time, currents exceeded 1.6 m/s and the turbine was generating power. The DAISY was equipped with a flow shield and passed directly over the turbine. A similar representation for a direct pass in somewhat lower currents with a shallow DAISY is shown in Figure 23 and highlights the once-per-rev click and shift in tonal frequencies with different rotation rate.

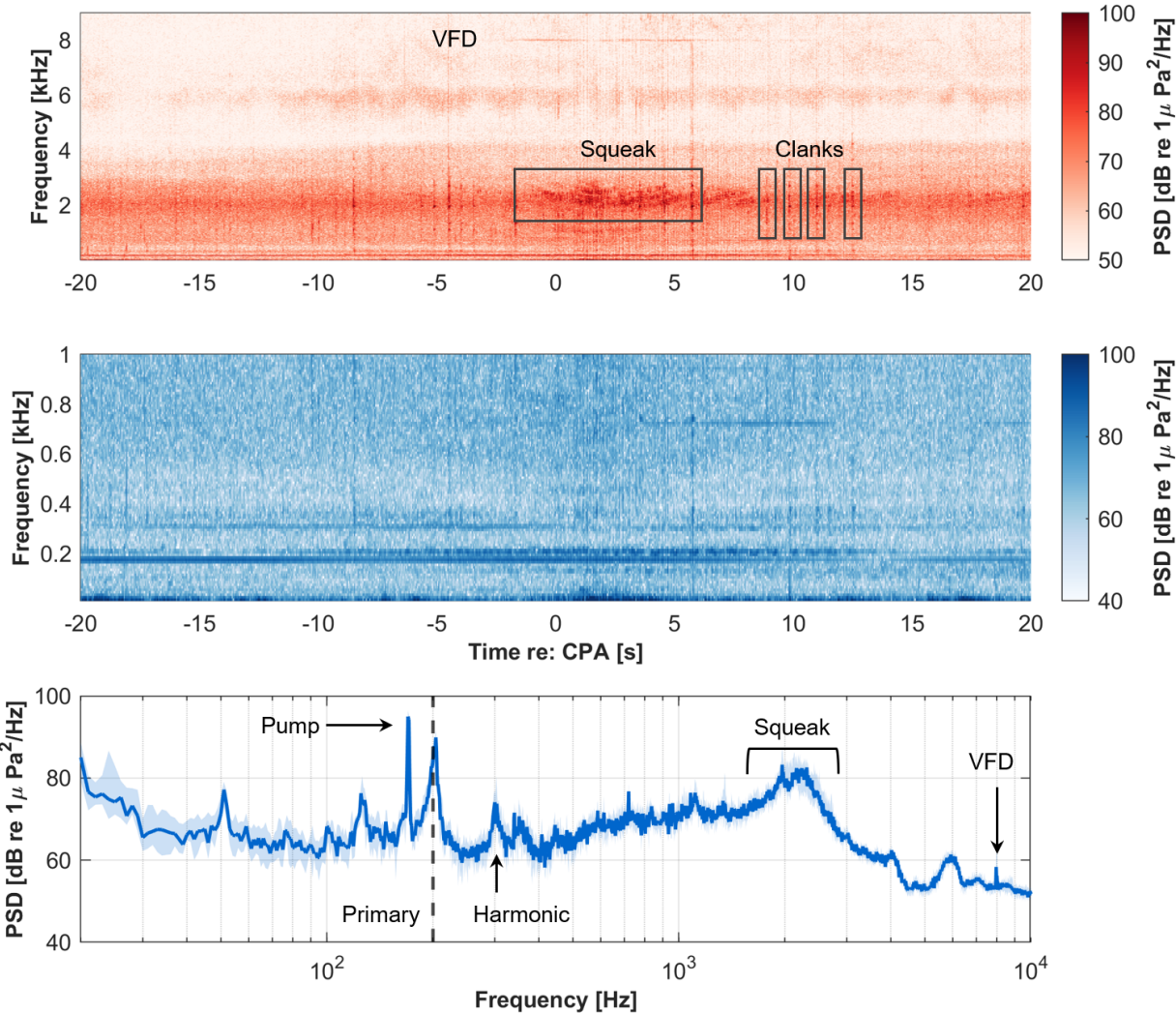


Figure 23: (a) Broadband and (b) low-frequency spectrograms annotated with acoustic events. The time axis is centered around the closest point of approach based on the estimated turbine location (likely within 2 m of actual). (c) Periodogram for 10 s surrounding the closest point of approach. Solid line denotes median and shaded region denotes interquartile range. The predicted primary tone associated with turbine rotation from dockside testing is indicated by the dashed line.

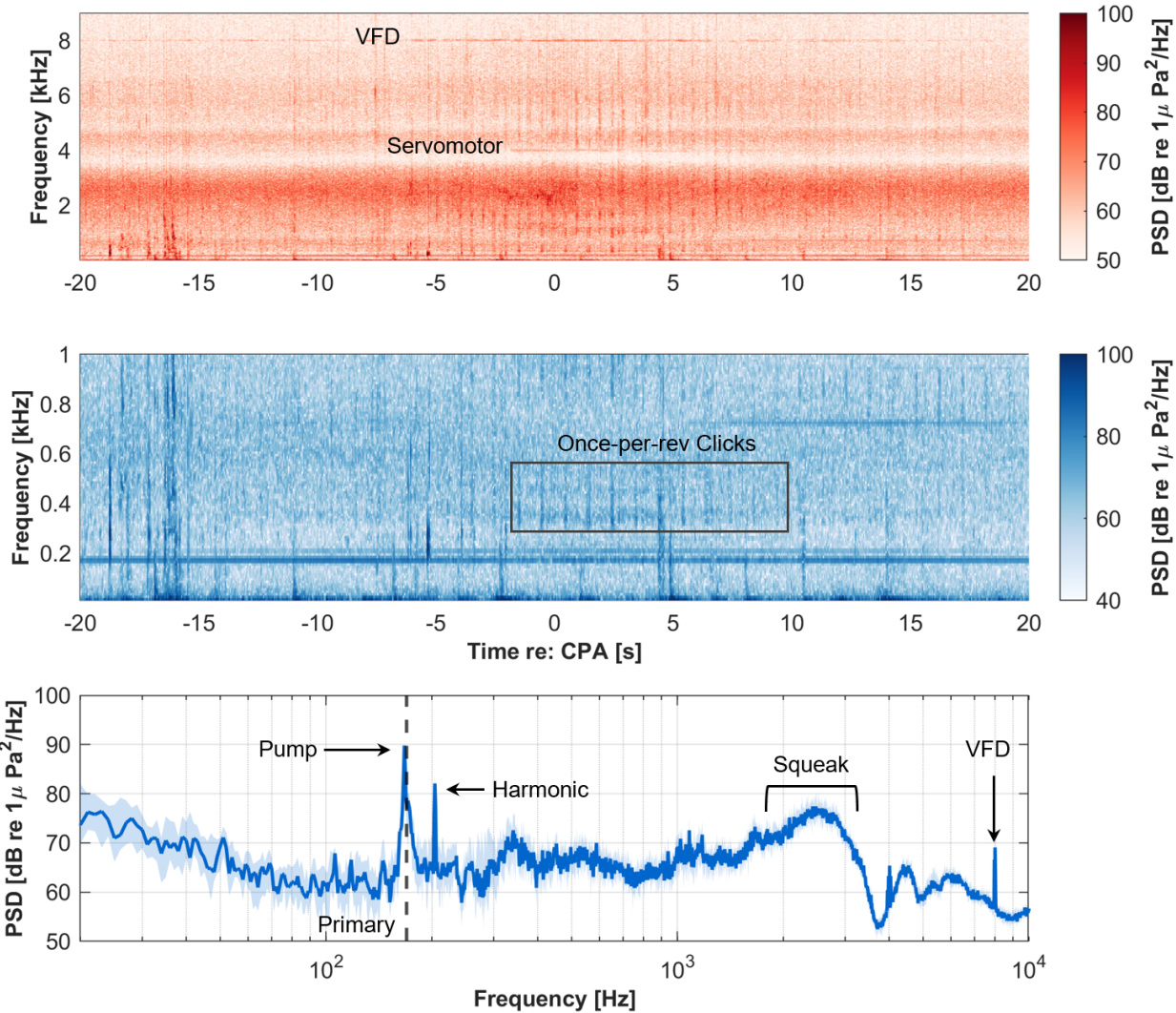


Figure 24: As for Figure 2, but during somewhat lower currents. Here, the primary tone associated with turbine rotation and pump frequency nearly overlap and the harmonics are shifted.

As shown in Figure 25, we observed an appreciable difference in received levels above 1 kHz that could not be entirely explained by range dependence or depth variation for the shielded and unshielded (shallow variant) DAISYs. As discussed in Polagye et al. 2024, we believe this is primarily a consequence of bubble adhesion to the inner and/or outer surfaces of the fabric flow shield. This is most likely to occur when flow shields are inserted into bubble-rich propeller wash of the deployment vessel. Because of the risk of running aground at night, the vessel held position against the currents, rather than free drifting, while DAISYs were deployed. This resulted DAISY passing directly through the propeller wash and this bubble cloud, which was apparent on the Lander active sonars and may have also had significant effects on sound propagation at higher frequencies (e.g., upwards refraction). We observe relatively limited differences in low-frequency (e.g., 10 Hz) received levels and relatively good agreement across all DAISYs at frequencies up to 1 kHz. The favorable low-frequency performance of the shallow DAISYs without flow shields is consistent with prior testing. Specifically, when there is limited shear between the

water surface and hydrophone depth, relative velocities between the hydrophone and surrounding water are minimal and flow noise for an unshielded hydrophone is substantially reduced.

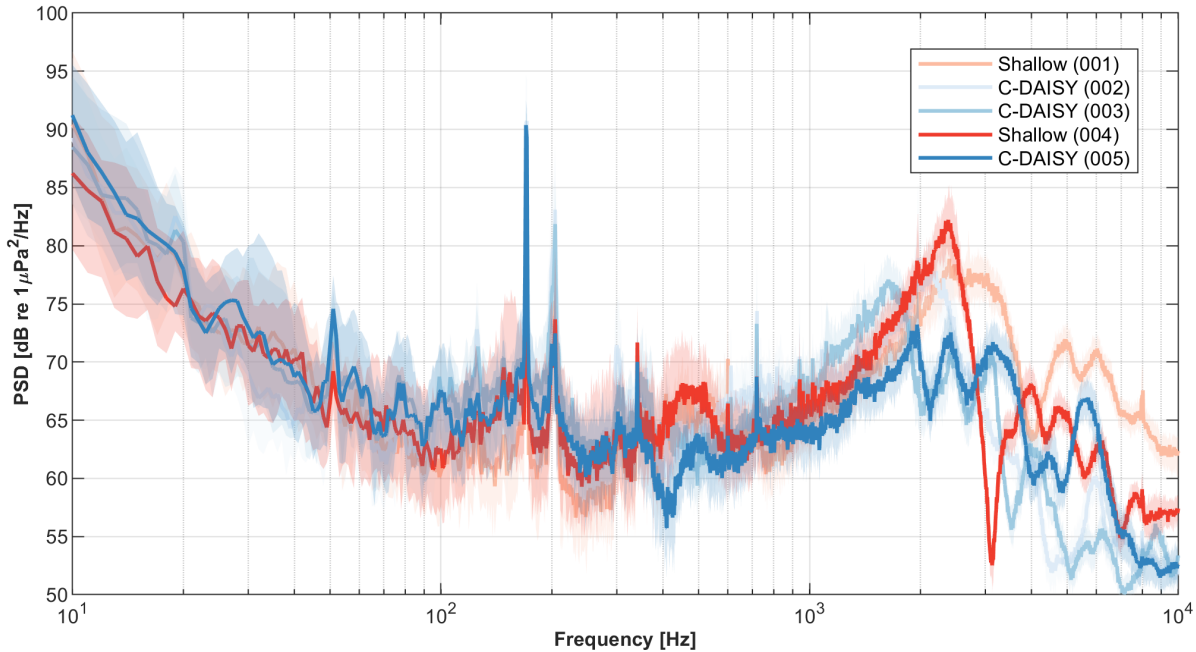


Figure 25: Co-temporal periodograms for all DAISYs in the same drift sequence as Figure 2. DAISY003 (C-DAISY) and DAISY 001 (Shallow DAISY) are nearly co-spatial.

Localization was attempted for “clanks”, “clicks”, and “squeaks” that might be attributable to the turbine. We were able to localize some of these events to the turbine (Figure 26), though this was often challenging. Specifically, localization is most accurate when a source with relatively high signal-to-noise is bracketed by a group of receivers. Because most turbine sounds only substantially exceeded ambient noise at relatively close range, in many cases these sounds were only apparent on one or two receivers, not the entire array. For the same reason, three-dimensional localization, which requires at least four receivers, did not produce reliable position estimates. However, localization to within 50 m was often possible (differentiating between the turbine and other sources of noise). Tones associated with the servomotor or turbine rotation could not be localized due to their time-invariant structure. Attempts to localize these types of sounds during turbine shutdown were also unsuccessful due to relatively low signal-to-noise ratios for most of the DAISY receivers. These factors mean that, while localization of relatively low-intensity noise sources is possible, this was more readily accomplished with vector sensors – albeit over a narrower frequency range than observable by the DAISYs.

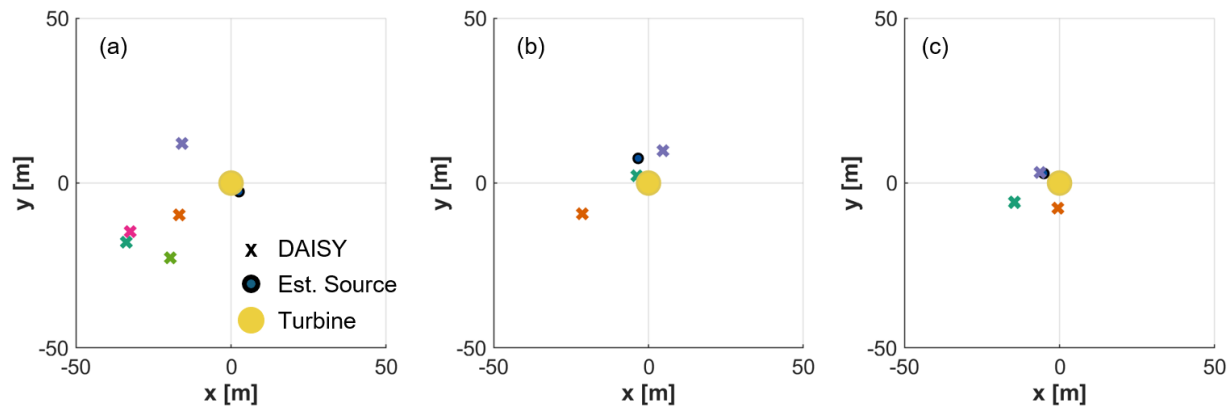


Figure 26: Examples of successful localization of (a) bearing squeak, (b) bearing “click”, and (c) clanking. (a) localized most accurately when using information from all five DAISYs, while (b) and (c) used information from the minimum number of receivers with the highest signal-to-noise ratios in the specified frequency range.

8.1.5 DAISY/Vector Sensor Comparison

Due to the loss of the first NoiseSpotter, we only had concurrent data from the PNNL vector sensor during DAISY drifts. DAISY drifts were targeted to drift over the NoiseSpotter®v1, so the DAISYs did not pass directly over the PNNL vector sensor (closest point of approach to PNNL sensor = 27 m). However, comparison between DAISY data and concurrent vector sensor data offers some insights into the accuracy and utility of both sensors. Figure 27 shows the mean power spectral density recorded by the PNNL vector sensor M20 pressure sensor and a DAISY during the closest point of approach. At the lowest frequencies measured (<80 Hz), the PNNL sensor reports higher amplitude than the DAISY. This can be attributed to flow noise affecting the stationary sensor, but not the drifting sensor. Between 80 and 500 Hz, measurements from the two sensors agree well. The peak amplitude of the 160 Hz tone associated with the water intake pump is 7 dB higher in the DAISY measurements; this can likely be attributed to different ranges from the intake. Tones associated with turbine are observed at the same frequencies. Above 500 Hz, the DAISY measurements are higher amplitude than the PNNL sensor. While this may be explained, in part, by different ranges from the turbine, it may also be related to an air bubble trapped in the flow shield (discussed in section 8.1.1).

While this project did not allow us to directly compare between all three sensors, subsequent comparison between DAISY and NoiseSpotter® v2 sensors conducted for another project in Newport, OR showed good agreement between 50 Hz and 2500 Hz, with divergences to either side of this associated with NoiseSpotter® signal filters.

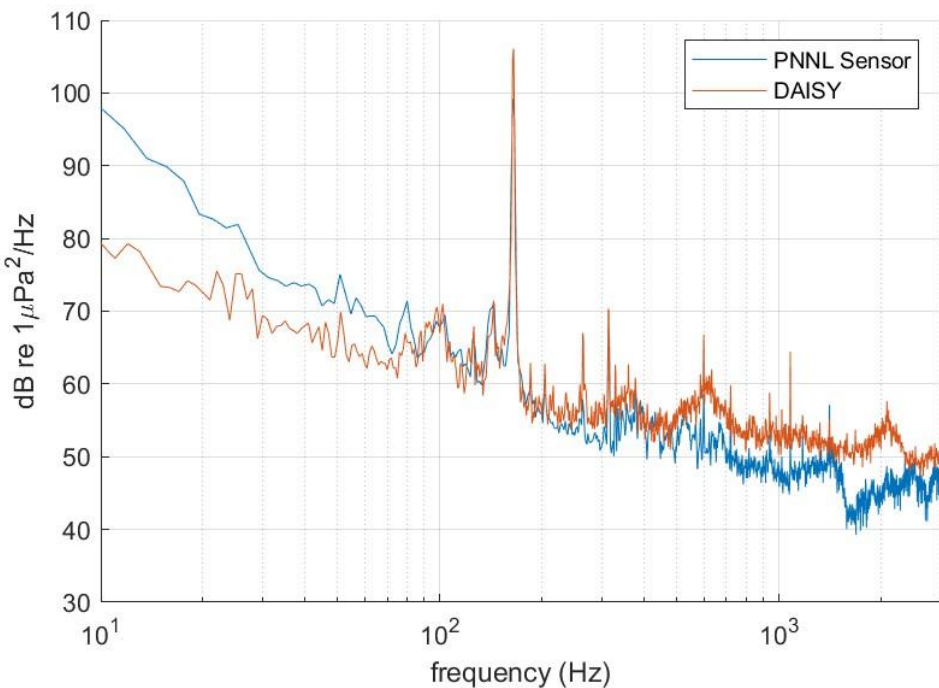


Figure 27: Mean power spectral density recorded by the DAISY and PNNL vector M20 pressure sensor during the four-second period when the DAISY was closest to the vector sensor (27 m range). The flow speed was 1.1 m/s at the turbine location during this time, and the turbine was rotating at 44 RPM.

8.2 Lesson Learned and Test Plan Deviation

The primary deviation from the test plan was the loss of the NoiseSpotter® following the first deployment at L2 and redeployment of a new NoiseSpotter® system several months later. The loss of the NoiseSpotter® and recorded data had several implications for the project:

- The only concurrent data from the PNNL sensor and the NoiseSpotter® are from the initial 1-day validation test with both sensors deployed near L1. Tidal currents did not exceed the turbine cut-in speed during this deployment, so the turbine was motored for a five-minute period. There are no concurrent data with the two sensor packages at different stations.
- Redeployment of a new NoiseSpotter® system occurred three months after the initial tests. By this time, one turbine blade had failed (turbine had three of four blades), and the turbine lost a second blade during the NoiseSpotter® deployment. Blade loss, biofouling, or other corrosion/fatigue on the system may have changed the radiated noise from the turbine relative to those recorded by the PNNL sensor.
- No data were collected at L3.

Despite extensive search efforts using divers, a drop camera, a sidescan sonar, and a remotely operated vehicle, as well as outreach to local boat operators, the first NoiseSpotter® remains lost. We do not know what caused the system to move from its original station but are confident that it is no longer in the area of the Sequim Bay tidal channel. Potential causes include 1) kelp or debris entangled on the platform, adding drag and causing it to overturn and drift away more easily, or 2) it was caught on the anchor or line from a passing vessel and dragged away. Given the exhaustive search of the interior of Sequim Bay,

the platform likely moved seaward and yet did not tangle on the Turbine Lander or its shore cable. Unfortunately, loss of sensors and data is always a risk with marine field operations, and we likely will never have a conclusive explanation for what caused the NoiseSpotter® to go missing. However, several lessons were learned that can reduce the risk of sensor loss or facilitate improved searching methods in the future:

- For the initial deployment, the NoiseSpotter® was anchored by lead weights on the platform. Screw anchors were added for the second, successful deployment for added security.
- A third-party company was contracted to conduct a search for the NoiseSpotter® with a sidescan sonar. While this was ultimately unsuccessful, it proved to be an efficient method for searching for the NoiseSpotter® and PNNL has since invested in a similar sidescan system optimized for use in shallow waters to augment testing capabilities.
- While we do not know if it would have allowed us to find the NoiseSpotter®, searching would have been aided by an ability to “ping” or communicate with the deployed platform. A PNNL acoustic release that can localize a deployed sensor was added to the second NoiseSpotter® lander, and “pinged” from the PNNL-Sequim pier once a day to ensure that the sensor had not moved. PNNL has since invested in an acoustic modem system that can be used for this purpose.

Actual sensor deployment locations deviated from the planned locations due to the inherent difficulty in dropping a sensor at an exact location from a vessel. Further, deployment locations near L1 were moved slightly north to minimize the risk of dropping a sensor package on the turbine cable. Shore GPS points of the cable location would have further reduced this risk and could be facilitated in the future by divers with the new PNNL acoustic modem system.

Our data analysis methodology also deviated slightly from the original test plan. There are two reasons for this: 1) this was the first data set of vector sensor data around a tidal turbine, necessitating some “data exploration” and fine-tuning of analysis methods to most effectively represent the data and 2) the sound from the turbine was faint compared to other sound sources in the area, making standard acoustic data processing methods difficult to implement.

Finally, the original test plan specified that all data analysis would take place in Python. While the Integral team used existing Python codes, the PNNL team ultimately developed processing codes in MATLAB, because more of the team is familiar with this coding language.

Several lessons were learned that can inform future acoustic measurements around marine energy converters. First, while the turbine sound was detected by the vector sensors, the sound was faint and difficult to localize and identify. Vector sensors were deployed at approximately 100 m range from the turbine following the IEC technical specification for acoustic characterization of marine energy converters, but data would likely have been more informative if the sensors were closer to the turbine. Based on DAISY measurements, the most prominent sounds attributable to the turbine were only apparent above background levels to a range of ~10 m. This result agrees with previous measurements of marine energy converter sound that have indicated that 100 m might be “too far” to characterize the sound from a device, particularly for small-scale marine energy converters.

While DAISYs had been deployed several times at MCRL during their development, this was the first attempt to do so at night (Figure 28). As discussed in Section 6.3, nighttime operations heighten hazards

associated with on water work. Because of this, going into the survey, it was uncertain if it would be possible to safely deploy even three DAISYs at a time, let alone five DAISYs for over-determined localization. We were, however, able to mitigate this risk successfully and, after a few initial drifts, had reduced the recovery-redeployment cycle for five DAISYs to less than 10 minutes. This was attributable to two factors: (1) all UW personnel had significant on-water experience with DAISY deployment and recovery, allowing the team to work together effectively and efficiently and (2) two PNNL operators were aboard, allowing one to focus on driving and the other to focus on spotting landmarks and relaying the status of operations on the deck.



Figure 28: DAISY Preparation during nighttime operations (credit: Shanon Dell, PNNL)

9 CONCLUSIONS AND RECOMMENDATIONS

This test characterized the sound produced by the Turbine Lander and demonstrated the utility of directionally-resolved acoustic measurements at marine energy sites. Analysis of vector sensor data readily identified the characteristics of sound generated by the turbine with more certainty than could be achieved with only hydrophones on the stationary platforms. Specifically, low amplitude sounds (like those of the camera wipers) could be attributed to the Turbine Lander and would likely have been overlooked in measurements from a single hydrophone. While deployment of vector sensors for all acoustic characterizations of marine energy converters is not feasible nor recommended, they can provide uniquely valuable information. First, vector sensors simplify the challenge of separating sounds from different sources and attributing sound to the device through directional processing from a single sensor. Second, vector sensors can directly measure particle motion levels, which can be used to understand potential auditory effects on fish. Finally, as demonstrated here, while it is possible to localize sound from a turbine of this size using an array of drifting hydrophones, more reliable localization can be achieved with vector sensors. Such localization is temporally persistent, allowing patterns between ebb and flood tide, as well as across deployments to be identified.

10 REFERENCES

Bassett, Christopher, Jim Thomson, Peter H. Dahl, and Brian Polagye. 2014. "Flow-Noise and Turbulence in Two Tidal Channels." *The Journal of the Acoustical Society of America* 135 (4): 1764–74. <https://doi.org/10.1121/1.4867360>.

Cotter, Emma, James McVey, Linnea Weicht, and Joseph Haxel. 2024. "Performance of Three Hydrophone Flow Shields in a Tidal Channel." *JASA Express Letters* 4 (1): 016001. <https://doi.org/10.1121/10.0024333>.

Dahl, Peter H., Julien Bonnel, and David R. Dall'Osto. 2024. "On the Equivalence of Scalar-Pressure and Vector-Based Acoustic Dosage Measures as Derived from Time-Limited Signal Waveforms." *The Journal of the Acoustical Society of America* 155 (5): 3291–3301.

Martin, S. Bruce, Briand J. Gaudet, Holger Klinck, Peter J. Dugan, Jennifer L. Miksis-Olds, David K. Mellinger, David A. Mann, et al. 2021. "Hybrid Millidecade Spectra: A Practical Format for Exchange of Long-Term Ambient Sound Data." *JASA Express Letters* 1 (1): 011203. <https://doi.org/10.1121/10.0003324>.

Polagye, Brian, Corey Crisp, Lindsey Jones, Paul Murphy, Jessica Noe, Gemma Calandra, and Christopher Bassett. 2024. "Performance of a Drifting Acoustic Instrumentation SYstem (DAISY) for Characterizing Radiated Noise from Marine Energy Converters." *Journal of Ocean Engineering and Marine Energy*, December. <https://doi.org/10.1007/s40722-024-00358-6>.

Popper, Arthur N., and Anthony D. Hawkins. 2019. "An Overview of Fish Bioacoustics and the Impacts of Anthropogenic Sounds on Fishes." *Journal of Fish Biology* 94 (5): 692–713. <https://doi.org/10.1111/jfb.13948>.

Tenorio-Hallé, Ludovic, Aaron M. Thode, Marc O. Lammers, Alexander S. Conrad, and Katherine H. Kim. 2022. "Multi-Target 2D Tracking Method for Singing Humpback Whales Using Vector Sensors." *The Journal of the Acoustical Society of America* 151 (1): 126–37. <https://doi.org/10.1121/10.0009165>.

Thode, Aaron M., Taiki Sakai, Jeffrey Michalec, Shannon Rankin, Melissa S. Soldevilla, Bruce Martin, and Katherine H. Kim. 2019. "Displaying Bioacoustic Directional Information from Sonobuoys Using 'Azigrams'." *The Journal of the Acoustical Society of America* 146 (1): 95–102. <https://doi.org/10.1121/1.5114810>.

Wahlberg, Magnus, Bertel Møhl, and Peter Teglberg Madsen. 2001. "Estimating Source Position Accuracy of a Large-Aperture Hydrophone Array for Bioacoustics." *The Journal of the Acoustical Society of America* 109 (1): 397–406. <https://doi.org/10.1121/1.1329619>.

11 ACKNOWLEDGEMENTS

The authors wish to acknowledge Garrett Staines, Tristen Myers, and John Vavrinec for their support of field operations and the search effort for the NoiseSpotter v1.